REPORT DOCUMENTATION PAGE

Form Approved
OMB No. 0704-0188

1. REPORT DATE *(DD-MM-YYYY)*	2. REPORT TYPE	3. DATES COVERED *(From - To)*
01062012	Final Technical	05-01-07 to 04-30-2011q

4. TITLE AND SUBTITLE
An AUV-Based Investigation of the Role of Nutrient Variability in the Predictive Modeling of Physical Processes in the Littoral Ocean

5a. CONTRACT NUMBER
n/a

5b. GRANT NUMBER
N00014-07-1-0800

5c. PROGRAM ELEMENT NUMBER

6. AUTHOR(S)
Fanning, Kent A.
Masserini, Robert T., Jr

5d. PROJECT NUMBER

5e. TASK NUMBER

5f. WORK UNIT NUMBER

7. PERFORMING ORGANIZATION NAME(S) AND ADDRESS(ES)
University of South Florida
140 - 7th Avenue, South
St. Petersburg, FL 33701

8. PERFORMING ORGANIZATION REPORT NUMBER
n/a

9. SPONSORING/MONITORING AGENCY NAME(S) AND ADDRESS(ES)
ONR Reg Admin Atlanta - N66020
100 Alabama Street SW, Ste. 4R15
Atlanta, GA 30303-3104

10. SPONSOR/MONITOR'S ACRONYM(S)

11. SPONSORING/MONITORING AGENCY REPORT NUMBER

12. DISTRIBUTION AVAILABILITY STATEMENT
DISTRIBUTION STATEMENT A: Distribution approved for public release; distribution is unlimited.

13. SUPPLEMENTARY NOTES

14. ABSTRACT
Progress was made in the design of instruments to perform high-sensitivity measurements of ammonium, nitrate, and nitrite in the upper ocean and in data analysis from field expeditions with those instruments. The Long-Term Goal is to use tiny nutrient changes as descriptors of geophysical fields in the upper ocean. Expedition data showed the importance of wind. Low wind stress led to large ammonium peaks. As wind stress increased, ammonium peaks weakened and then disappeared. Thus the features of ammonium peaks are descriptors of wind effects on the condition of the surface ocean. The Masserini/Fanning lab nutrient sensor was adapted for a Bluefin-type AUV and then modified further into a robust lightweight pulsed xenon fluorescence nutrient analyzer that is cheap and can work on smaller boats. The importance of this new analyzer will be its ability to make possible the large number of surveys necessary to follow the occurrence and fate of ammonium peaks. Finally, initial evaluations of the ISUS ultraviolet-based nitrate sensor indicated that it can function in our coastal waters but has problems and is not very sensitive.

15. SUBJECT TERMS
Ammonium, nitrate, nitrite, fluorescence, wind speed, wind stress, peak, duration time, background concentration, maximum, standard curves, reagent blanks, weather front

16. SECURITY CLASSIFICATION OF:			17. LIMITATION OF ABSTRACT	18. NUMBER OF PAGES	19a. NAME OF RESPONSIBLE PERSON
a. REPORT	b. ABSTRACT	c. THIS PAGE	UU	19	Kent A. Fanning
U	U	U			19b. TELEPONE NUMBER *(Include area code)* 727-553-1584

Final Technical Report:

An AUV-Based Investigation Of The Role Of Nutrient Variability In The Predictive Modeling Of Physical Processes In The Littoral Ocean

Grant Number: N00014-07-1-0800

Principal Investigators:

Dr. Kent A. Fanning
College of Marine Science
University of South Florida
St. Petersburg, FL 33701
phone: (727) 553-1594
email: kaf@marine.usf.edu

Dr. Robert T. Masserini, Jr.
College of Marine Science
University of South Florida
St. Petersburg, FL 33701
phone: (727) 553-1646
email:masserin@marine.usf.edu

Long-term Goals:

Our long-term goal is to evaluate the utility of low-level concentrations of nitrate, nitrite, and ammonium as tracers of physical processes in oligotrophic coastal waters and as descriptors of geophysical fields. To facilitate this goal, a primary focus has been adapting our laboratory sensor for use in an autonomous underwater vehicle (AUV). In addition to further work on an AUV version, a new focus for this grant was to construct a compact lightweight version of the Masserini/Fanning (2000) sensor that can operate from smaller and cheaper research vessels. Use of this version, by itself or in conjunction with an AUV version, will permit much more frequent and detailed monitoring of low-level nutrient spikes in coastal waters. The utility of tiny increases in nitrogenous nutrients for detecting manmade benthic disturbances in coastal waters is an important component of our research since these increases can also be tracers.

Biological processes produce variations in nutrient concentrations throughout the ocean. Usually, the biggest differences in nutrient concentrations occur between surface water and deep water or between one mass of deep water and another mass of deep water. These differences have been utilized for some time to identify and track deep-water masses, but the surface ocean is different. Surface nutrient concentrations in most of the oceans tend to be low, so low in fact that the standard nutrient techniques (e.g., Gordon et al., 1993) have detection limits that are approximately the same magnitudes as the concentrations, thus precluding the detection of surface-water concentration differences. However, we developed a high-sensitivity fluorescent sensor for three of those nutrients (nitrate, nitrite, and ammonium) that had detection limits considerably lower than their surface nutrient concentrations (Masserini and Fanning, 2000). This sensor offers the exciting prospect of using these nutrients as "tags" for masses of surface water that will track those masses when conventional measures like temperature and salinity might not. Further, a miniaturized Masserini-Fanning sensor operating independently in an AUV to obtain *in situ* nutrient measurements could thus evaluate the horizontal sizes and distributions of surface seawater masses through simultaneous mapping efforts with the shipboard version of

 20120718145

the Masserini-Fanning sensor. The AUV version would also permit much greater coverage of nutrient-enriched boluses in deeper layers within the surface ocean, which can now only be studied by the much less definitive process of CTD rosette hydrocasts.

We also began to evaluate the feasibility of using ISUS ultraviolet *in situ* sensors in long-term monitoring of nitrate inputs to coastal waters and nitrate pulses near shore.

This report presents our progress toward these long-term goals.

Lagrangian Experiments On Surface Ammonium Events

Two Lagrangian experiments on ammonium (NH_4^+) were conducted using sulfur hexafluoride to label surface water masses. The site of the experiments (FSLE V and FSLE VI) was the low-nutrient euphotic zone in continental-margin waters of the eastern Gulf of Mexico (Fig. 1). The biogeochemical cycling of nitrate, nitrite, and ammonium were monitored within the labeled regions over the course of the experiments. The methodology, experimental details, and results previously reported in the Final Technical report for grant N00014-02-1-0240 are summarized here, followed by the more recent data analysis conducted under this grant. The resultant wind speed, barometric pressure, and ammonium data for FSLE V and VI are presented in Figures 2 and 3, respectively.

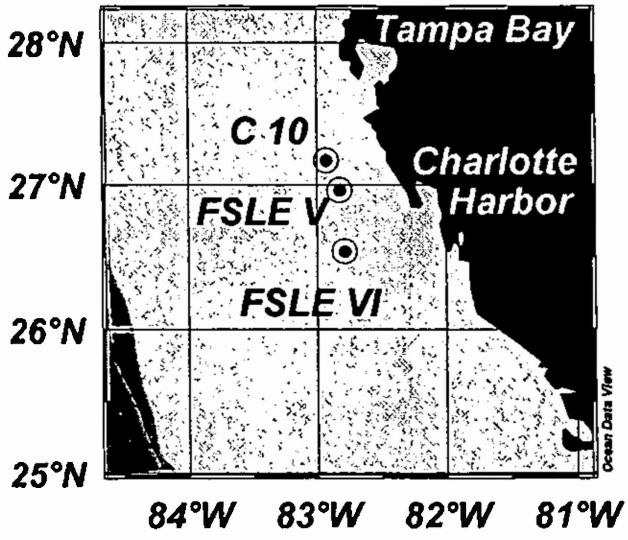

Fig. 1. Locations of SF_6 injection sites for the FSLE V and FSLE VI experiments in the eastern Gulf of Mexico in April, 2001 and November, 2002, respectively. The SF_6-labeled surface seawater tended to drift southward during the experiments, in accord with the general circulation patterns (Weisberg et al. 2009). The location of a nearby current-meter mooring with meteorological instrumentation (C10) is also shown; C10 is part of the West Florida Shelf mooring array maintained by the University of South Florida COMPS program (http://comps.marine.usf.edu/

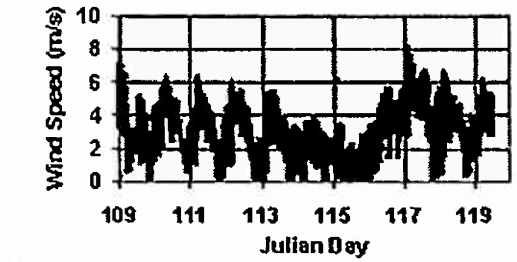

a

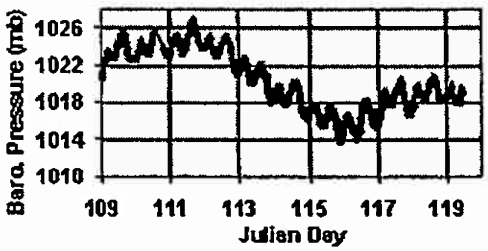

b

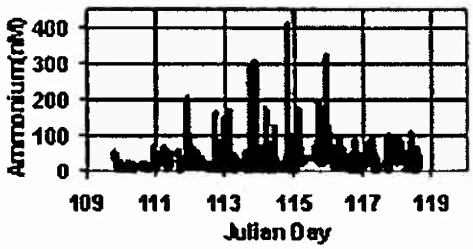

c

Fig. 2. Time courses of wind speed (a), barometric pressure (b), and NH_4^+ concentration (c) in the upper 2 meters of the ocean during the FSLE V experiment on the West Florida continental shelf between Julian Days 110 and 118.5 in April, 2001. Wind speeds, measured by an anemometer on the research vessel (F.G. Walton Smith) and corrected for ship's speed and direction, agree with the regional patterns from measurements on COMPS mooring C10 (Fig. 1). NH_4^+ concentrations, measured on seawater flowing into the dedicated seawater system of the research vessel, show the presence of maxima as "peaks" above background NH_4^+ concentrations (0-80 nmol L^{-1}).

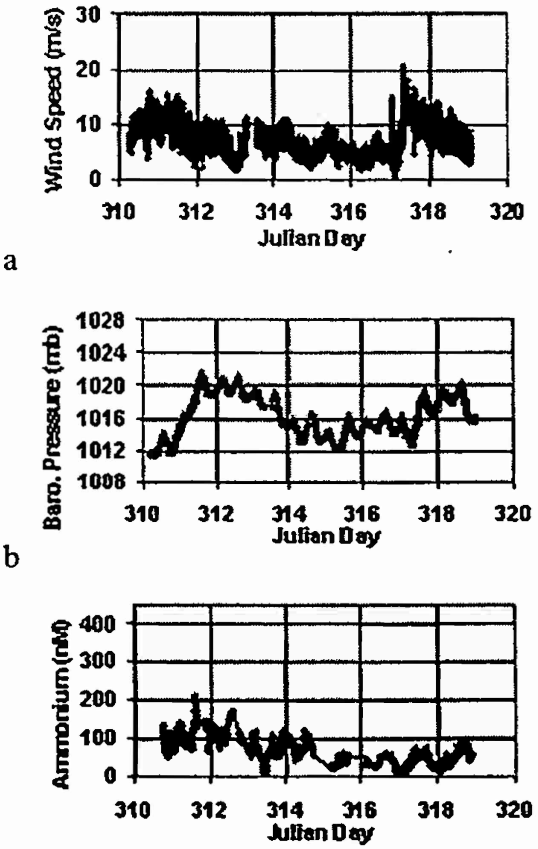

Fig. 3. Time course of wind speed (a), barometric pressure (b), and NH_4^+ concentration (c) in the upper 2 meters of the ocean during the FSLE VI experiment on the West Florida continental Shelf between Julian Day 310.5 and 319 in November, 2002. Wind speeds, measured by an anemometer on the research vessel (F.G. Walton Smith) and corrected for ship's speed and direction, agree with the regional patterns from measurements on COMPS mooring C10 (Fig. 1). NH_4^+ concentrations, measured on seawater flowing into the dedicated seawater system of the research vessel, show the presence of maxima as "peaks" above background NH_4^+ concentrations (0-80 nmol L^{-1}).

The principal observations of our two-experiment field study were the ammonium event (= a clustering of enriched ammonium concentration peaks) during FSLE V and the lack of an ammonium event during FSLE VI. Unfortunately though, the patterns of several commonly measured environmental parameters in the water column provided little help in explaining either one. Salinity ranges were nearly identical: FSLE V (36.37-36.56) vs. FSLE VI (36.28-36.39), as were fluorometric chlorophyll values: FSLE V (0.08-0.60 μg l^{-1}) vs. FSLE VI (0.07-0.41 μg l^{-1}). Temperatures on FSLE VI (26.32-27.42°C) were warmer than on FSLE V (19.62-22.70°C), but this difference was most likely unimportant.

The only other available environmental parameters in FSLE V and FSLE VI were meteorological, and examination of the time courses of wind speed and barometric pressure suggested a plausible explanation of the ammonium features and trends in both experiments. During FSLE V, variations in meteorological parameters, as measured on shipboard (Fig. 2a and

b) and confirmed for the study region by instruments on mooring C10 (Fig. 1), appeared to coincide with the presence or absence of [NH_4^+] maxima (Fig. 2c). From JD 110 through part of JD 111, wind speeds were mostly ~1 ms^{-1} to ~7 ms^{-1}, while barometric pressure was 1022-1027 mb. But, near the end of JD 111, both parameters began to change. Wind speeds decreased, with minimum values becoming ≤ 1 ms^{-1} for increasingly long periods of time and maximum wind speeds declining, eventually to ≤ 4 ms^{-1} at JD 114 – 116. Barometric pressure decreased to 1014 -1019 mb. Then both wind speed and barometric pressure increased rather sharply, mostly during JD 116. These wind-speed and barometric-pressure patterns indicate the approach and passage of a low-pressure weather front (Virmani and Weisberg 2005). The period of calming winds ahead of the front was of particular interest because it coincided so closely with the period in which the strong [NH_4^+] maxima were present -- i.e., the ammonium event in Fig. 2c during JD 112-116. When wind speeds and barometric pressure subsequently increased during frontal passage on JD 116, the maxima, and the event, disappeared.

Winds generate sea-surface wind stress, enhancing turbulence. The natural clumping of planktonic organisms into patches is well known (Martin 2003), and ammonium concentrations should be higher in patches abundant with bacteria and other organisms responsible for ammonium release during organic-matter remineralization. Faster wind speeds lead to greater wind stress and should produce more intense mixing between such patches and the surrounding seawater, resulting in the dispersion of the organisms and the dilution of the ammonium concentrations.

Once wind speeds weaken -- for example preceding an approaching low-pressure front -- mixing should also weaken, and the concentrations of the remineralization-producing organisms and the NH_4^+ they release would be expected to increase within patches. Each FSLE V [NH_4^+] maximum in the ammonium event (Fig. 2c) appeared as a coherent bolus or "patch" with a peak in concentration . Distances across these peaks, estimated from the positions of the beginnings and endings of the peaks, were 1.1-4.4 km, or in the low end of the mesoscale/sub-mesoscale range (1-100 km) that describes features like filaments, eddies, etc. customarily considered as patches (Martin 2003).

Wind behavior can also explain the disparity between FSLE V results and FSLE VI results, even though a preliminary examination of Fig. 3 (a and b) suggests that the weather pattern of FSLE VI in fact resembled that of FSLE V. The decline of wind speed and barometric pressure between JD 311.5 and JD 317, followed by strong increases in both parameters, clearly denotes the approach and passage of a weather front (Virmani and Weisberg 2005) during FSLE VI, just as seen in FSLE V -- Fig. 2 (a and b). FSLE VI might thus have been expected to exhibit an ammonium event with [NH_4^+] maxima ≈ 400 nmol L^{-1}. However, closer examination reveals a fundamental difference: FSLE VI wind speeds were considerably higher than FSLE V wind speeds. (Notice the difference between the wind-speed scales in Figs. 2a and 3a). FSLE V wind speeds frequently dropped to zero, especially during JD 114-116, when the ammonium peaks were particularly strong (Fig. 2c), and were never above 8.2 ms^{-1}. In contrast, FSLE VI wind speeds were often >10 ms^{-1}, and even reached 15-22 ms^{-1} (Fig. 3a).

The differing effects of wind in FSLE V and FSLE VI are highlighted by two types of analysis: average daily wind speeds and dispersion estimates.

Calculations on wind data from the *RV F.G. Walton Smith* demonstrated the different potential impacts of wind speed during FSLE V and FSLE VI (Table 1). The approach was to calculate time patterns in wind speed for each experiment, beginning even before the first instances (called time zero in Table 1) when loci of maxima in SF_6 concentration were first identified within the SF_6-labeled areas of seawater. The average daily wind speed was calculated for a 12-day period in FSLE V and a 9-day period in FSLE VI. The much greater wind impact in FSLE VI is clearly evident. During FSLE V, the highest average daily wind speed was 6.3 ms^{-1}, and all but two of the average daily wind speeds in FSLE VI are larger than that. The lowest average daily FSLE V wind speeds of ~1 ms^{-1} occurred on JD 114-115, during the calm period before frontal passage, and were coincident with the ammonium event (Fig. 2c). In contrast, the approximately five-fold higher lowest average daily FSLE VI wind speeds occurred on JD 315-317, during the calm period before frontal passage, and were coincident with ammonium concentrations that were essentially at background levels (Fig. 3c).

Table 1. *Average daily wind speeds calculated from shipboard, motion-corrected anemometer data on R/V F. G. Walton Smith during the FSLE V and FSLE VI experiments. Time values from Fig. 2 (a-c) and Fig. 3 (a-c) are presented for comparison, and the corresponding Julian days are also presented.*

FSLE V			FSLE VI		
Julian Day	Time in Fig. 2 (d)	Average daily wind speed (ms^{-1})	Julian Day	Time in Fig. 3 (d)	Average daily wind speed (ms^{-1})
108		6.3	310		10.2
109		2.8	311		8.9
110	0	3.8	312	0	6.7
111	1	3.1	313	1	6.7
112	2	3.1	314	2	6.4
113	3	2.7	315	3	5.9
114	4	1.9	316	4	4.8
115	5	0.9	317	5	9.2
116	6	3.5	318	6	8.0
117	7	4.6			
118	8	3.5			
119	9	4.1			

The interactions of wind with the sea surface, which are important for dispersion processes as well as gas exchange with the atmosphere, can be quite sensitive to differences in wind forcing, such as presented in Table 1. Sea-surface wind stress (a parameter related to frictional effects of wind on these processes) typically varies with the magnitude of the wind speed raised to a power on the order of two (Neumann and Pierson 1966). After SF_6 injection into a seawater parcel, SF_6 concentration will decline because of atmospheric gas exchange and because the water parcel disperses into its surroundings and mixes with those waters, in which the SF_6 concentration is zero. This dispersion and mixing will also tend to reduce any maximum in $[NH_4^+]$ because $[NH_4^+]$ is lower in the seawater surrounding the maximum. SF_6 can thus serve as a "proxy" for NH_4^+ in evaluating the effects of dispersion and mixing, once corrections for SF_6 gas exchange are applied.

Wind forcing enters this exchange evaluation as the square of the wind speed when the SF_6 gas exchange coefficient (k) is calculated using coefficients derived from the gas transfer of oxides of stable carbon and radiocarbon (Wanninkhof 1992). The net air-sea SF_6 gas exchange flux (F) is proportional to the difference between the concentration of SF_6 in the seawater (C_w) and the

concentration of SF_6 in air (C_a). But, since C_a may be assumed to be zero, $F = k \bullet C_w$, which makes the flux a first-order process. Consider a volume of seawater (V) of area "A" and average depth "h" in the ocean's mixed layer. Now $V = A \bullet h$; so the total mass of SF_6 gas in the seawater is $M = V \bullet C_w = A \bullet h \bullet C_w$. The net flux F of SF_6 across the air-sea interface -- in mass/unit area/unit time (t) -- is then given by:

$$F = (A)^{-1} \bullet dM/dt = h \bullet dC_w/dt = k\,(C_w),$$

where C_w = the concentration of SF_6 remaining in the seawater at time = t, and dC_w/dt = rate of decline in SF_6 concentration in the mixed layer volume V due to loss to the atmosphere. Integration of "$h \bullet dC_w/dt = k\,(C_w)$" yields:

$$C_w/C_{wo} = \exp\,(k \bullet h^{-1} \bullet t) = f_{exch} \qquad \text{(Eq. 1)},$$

where $C_w/C_{wo} = f_{exch}$ represents the fraction of the original SF_6 concentration (C_{wo} at time = 0) remaining in seawater volume V after gas exchange has occurred for a time period = t. Of course, dispersion has occurred during the same time period, and thus the fraction of the original concentration of SF_6 remaining after gas exchange (f_{exch}) has been reduced further by another fraction that represents the effect of dispersion: f_{disp}. The actual measured value of C_w is significantly less than the C_w value that would be present if only gas exchange were occurring, and the actual measured fraction of the original concentration of SF_6 that remains after time t (f_{total}) is given by: $f_{total} = f_{exch} \bullet f_{disp}$. This equation may be rearranged to solve for f_{disp} as follows:

$$f_{disp} = f_{exch} \bullet (f_{total})^{-1} \qquad \text{(Eq. 2)}$$

As discussed below when presenting the work of Johnson et al. (2008), ammonium need not be assumed to undergo a significant gas-exchange process with the atmosphere at the time scales considered here. So the only physical process that could reduce ammonium concentration may be assumed to be dispersion, and values for f_{disp} obtained for SF_6 would also apply to any solute, e.g., ammonium. The measure of the impact of the dispersion that affected ammonium concentrations in surface waters during the FSLE V and FSLE VI experiments was obtained from the changes in the SF_6 concentration present at different times after time zero. Once time zero was selected for each experiment, the values of f_{exch} at different times (t) were calculated from Eq. (1), where k was obtained from Eq. (3) of Wanninkhof (1992) utilizing wind-speed data from the *R/V F.G. Walton Smith*. The average water depth (h) in Eq. 1 was taken to be 25 m. The field protocol on both experiments was to survey the SF_6-labeled regions of surface water in a manner that could identify the loci of maximum SF_6 concentrations within them at the values of "t" that corresponded to calculated values of f_{exch}. These loci identified the approximate centers of the dispersing SF_6, with time zero in each experiment being established when the first sampling of the center of the labeled area occurred. Division of these maximum concentrations by the initial SF_6 concentrations in the centers of the labeled areas at time zero yielded the values of f_{total} corresponding to the f_{exch} values, and Eq (2) was then used to calculate the values of f_{disp} that described the dispersion of ammonium ions in the labeled areas during FSLE V and FSLE VI.

A comparison of the temporal trends of ln f_{disp} against time (Fig. 4) indicated that dispersion was distinctly different in the two experiments. The magnitude of the negative slope of ln f_{disp} vs

time was 68% larger for FSLE VI than for FSLE V. Thus, after 3 days, the fraction of SF_6 remaining in the center of the FSLE V labeled area was ~2 times greater than in the FSLE VI labeled area. After 6 days the fraction of SF_6 remaining in the center of the FSLE V labeled area was ~4 times greater than in the FSLE VI labeled area. These estimates indicate a much greater

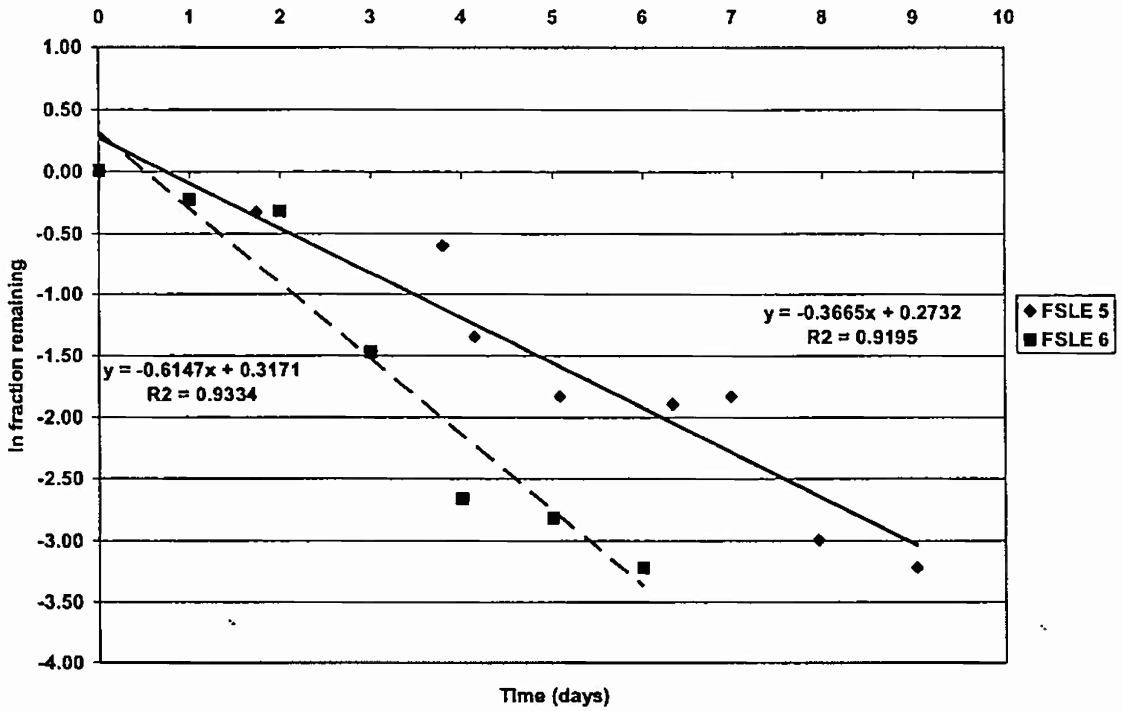

Fig. 4. The time variation of the natural logarithm of the mass fraction of SF_6 (f_{disp}) remaining in the centers of the SF_6-labeled areas of coastal water during the FSLE V and FSLE VI experiments after correction for SF_6 loss due to gas exchanges with the atmosphere. f_{disp} is also a measure of the relative reduction in ammonium concentrations as a result of dispersion (mixing) processes during FSLE V and VI (see text).

dispersion for the FSLE VI experiment, affecting both SF_6 and ammonium concentrations. Overall then, wind-regime comparisons indicated that average daily wind speeds were up to 10-fold higher and wind-driven dispersion of ammonium was accordingly 2-4 times higher in FSLE VI than in FSLE V.

The duration of the FSLE V ammonium maxima and the possible sources of the ammonium that formed the maxima are also important aspects to consider.

Under many circumstances, marine phytoplankton prefer ammonium over nitrate as a nitrogen source (Dortch 1990). Utilization of ammonium requires less energy since its nitrogen is fully reduced and is an immediate precursor to amino-acid nitrogen. Nitrate, by contrast, requires reduction by eight electrons per ion in order to be as usable (Hildebrand 2005). So an obvious question to ask is, "Given that ammonium is such a critical nutrient, should we not have expected the phytoplankton in Gulf of Mexico surface waters in the FSLE V experiment to consume any remineralized ammonium as fast as it appeared, with the result that duration times of ammonium

concentration maxima or "peaks" would be effectively zero?" As part of a study of *Trichodesmium* species, ammonium uptake rates by phytoplankton were measured in those waters during 2001-2002 – see Table 6 of Mulholland et al. (2006). These rates can be used to estimate the duration times of the FSLE V ammonium maxima and thus address the question. The Mulholland et al (2006) uptake rates ranged from 6 to 67 nmol L^{-1} /hr when the red-tide organism *K. brevis* was absent (as was true during FSLE V). The largest FSLE V ammonium maximum was 434 nmol L^{-1}, or 354 nmol L^{-1} above the highest observed background concentration: 80 nmol L^{-1}. Thus, if we ignore any ammonium production that may have occurred during the sampling transect across that maximum, it would have been reduced to background in t = 354 nmol L^{-1} /(6 to 67 nmol L^{-1}/hr) = 5.3 to 59 hr. Similarly, a FSLE V ammonium maximum of 200 nmol L^{-1} is 120 nmol L^{-1} above the same background and would have been reduced to background in t = 1.8 to 20 hr. These ranges provide estimates of the duration times of the ammonium maxima in FSLE V, but are most likely underestimates since ammonium production was ignored.

The field-sampling protocol utilizing the Masserini-Fanning system was able to transect and fully define all ammonium peaks in 0.17 to 0.97 hr. Since these transit times are much smaller than the estimated peak duration times, ammonium uptake by primary producers was not rapid enough to prevent the peaks from being detected. In fact, the longest estimated ammonium peak duration times compare favorably with the entire 4-day interval between JD 112 and JD 116 when the ammonium event occurred in FSLE V (see Fig. 2c). If we make the reasonable assumption that ammonium production was also occurring, then some of the larger peaks (i.e., ammoniuin enrichments) should have persisted during most of that interval. The duration times of the ammonium peaks in FSLE V were far from zero.

Another question concerns the source(s) of the ammonium in the maxima observed during FSLE V, once again keeping in mind that no red tide (i.e., *K. brevis*) was present. Within the water column, two such sources are possible: dissolved organic nitrogen (DON) and particulate organic nitrogen (PON). DON concentrations determined by the Solorzano and Sharp (1980) and Valderama (1981) methods in the same Gulf of Mexico surface waters in 2002 (when red tide was also absent) averaged 8300 ± 1200 nmol L^{-1}. Although no DON values were measured during 2001, the 2002 results matched reasonably well with later DON results for the same waters when red tide was absent in 2004: 9100 ± 500 nmol L^{-1}. So it would be reasonable to assume that the DON concentration in the FSLE V experimental area is typically ~8000 nmol L^{-1} in the absence of red tide. Next, data on PON from CHN analyses in April 2001 averaged 3250 ± 1750 nmol L^{-1}, making the estimated total concentration of DON + PON during FSLE V equal to 11,250 nmol L^{-1}. Thus an ammonium release sufficient to produce the highest observed ammonium enrichment above background during FSLE V (354 nmol L^{-1}) would have required that only 3% of the total available organic nitrogen in the water column be remineralized by ammonifying organisms.

A study of air-sea exchanges of $NH_{3(g)}$, the volatile form of total dissolved ammonia, by Johnson et al. (2008) raises the issue of these exchanges as possible atmospheric sources for dissolved ammonium in the upper ocean. The potential significance of these fluxes to the ammonium-event study may be assessed as follows. Johnson et al. (2008) estimated the magnitudes and directions of $NH_{3(g)}$ exchanges at different latitudes and temperatures in the Atlantic. They

concluded that warm ocean temperatures at latitudes of 20-30°N, such as encountered at FSLE V and VI, tended to make seawater a net *source* of $NH_{3(g)}$ to the atmosphere. This conclusion suggests that the atmosphere could not have been the source of dissolved ammonium maxima, such as found during FSLE V.

But could the upward ammonium fluxes have caused a reduction in the magnitudes of the maxima in FSLE V? A typical $NH_{3(g)}$ flux for 20-30 °N latitude is 50 pmol m^{-2} s^{-1} -- Johnson et al. (2008), Fig. 6 and Fig. 7. This rate of loss would reduce the ammonium concentration in the top cubic meter by approximately 4 nmol L^{-1} per day. However, the CTD hydrocasts conducted during FSLE V found that the thicknesses of the boluses containing ammonium enrichments during the ammonium event were on the order of 5 meters. Therefore, a more appropriate calculation would consider the top five meters of the water column. If we assume that the upward ammonium flux affects the total ammonium concentration in the upper 5 meters of the ocean, it would deplete that concentration at a rate of 10 fmol l^{-1} s^{-1}. At this rate, the sea-to-air flux of $NH_{3(g)}$ would require ~400 days to consume the 354 nmol L^{-1} maximum above background in FSLE V. If the flux were doubled, it would require ~200 days to consume the 354 nmol L^{-1} FSLE V maximum. The lifetimes of the FSLE V maxima appear to on the order of 5 days, and the magnitudes and time scales associated with measured FSLE maxima seem to have been very different from those of air-sea ammonia fluxes. Based on data available then, the magnitudes and time scales of the upward air-sea ammonium fluxes estimated by Johnson et al. (2008) would appear to be too small to have had a meaningful impact on the FSLE V ammonium maxima. This finding supports the assumption that loss of ammonium to the atmosphere is negligible when using Eq. 2 (above) to estimate the ammonium dispersion coefficient, f_{disp}.

The implication of these results relates to the mechanism of recycled primary production in the ocean, for which ammonium is a critical nutrient. The fact that weakening winds might lead to substantial relative ammonium enrichments over time periods of days suggests a mechanism whereby planktonic primary producers can, in effect, receive localized ammonium "supplements" that then stimulate photosynthesis, and carbon fixation rates, to rise above their normal magnitudes at background ammonium levels.

Wind-influenced ammonium enrichments could be rather frequent. Each year the eastern Gulf of Mexico receives on average 7-8 winter storm fronts (Virmani and Weisberg 2005) such as observed in FSLE V and VI, and 24-hour, low-pass filtered hourly wind-speed data from the nearby COMPS current mooring C10 (Fig. 1) established that wind speeds persisted below 4 ms^{-1} for two days or more 72 times in 2001, suggesting ample opportunities during a year for calming winds to permit ammonium accumulation. Sixty-four percent of these opportunities occurred in May-August, the warmer and wetter season. These results point to wind-related ammonium events as part of a mechanism for enhancing the rate of oceanic ammonium cycling. The implication is that calm winds occurring throughout the ocean from time to time may thus lead to pulses of euphotic-zone ammonium enrichments. *The estimated lifetimes of these pulses suggest that pulse features and distribution may serve as an indicator of the smaller-scale impact of wind stress in the surface ocean. Too much wind stress obliterates ammonium peaks. As wind stress weakens, ammonium peaks begin to appear and mark the areas impacted by the weakening. With further wind stress weakening, ammonium peaks grow very large and may help to identify large "patches" of surface seawater wherein organisms may be concentrated. These*

discoveries provide the rationale behind the idea of using our nutrient sensor (s) to map the horizontal distribution of surface water masses mentioned in the Long Term Goals section above.

Other ramifications of ammonium events are worth considering in view of the modeled importance of nitrification in the oceanic euphotic zone (Yool et al. 2007), the possible changes to surface wind-stress in a warming climate (Vecchi and Soden 2007), the potential importance of air-sea ammonia fluxes (Johnson et al. 2008), and the long-standing question of the principal drivers of carbon fixation in the low-nutrient, oligotrophic ocean.

Progress On Designing and Constructing an AUV Version of the Masserini/Fanning Nutrient Sensor

Under the previous grant (N00014-02-1-0240), we developed a robust submersible analyzer that would accurately elucidate the distribution of nitrate, nitrite, and ammonium within oligotrophic systems simultaneously with high resolution, both temporally and spatially, and with detection limits of less than 20 nM for all three nutrients. However that AUV version of our nutrient sensor was designed for Florida Atlantic University's Ocean Explorer (OEX) AUV, which then became unavailable to us. So we remodeled the AUV version with a form factor similar to that of the *Bluefin* AUV. The repackaging work for this objective was designed to prepare the sensor for future *in situ* testing. A modular 10.5-inch diameter framework was fabricated to hold the sensor components inside the payload cowling of a Bluefin AUV. Integration of the new sensor power system and electronics with the original pump and valve module required a significant amount of effort due to the failure of the brushless dc motor that drives the pump-head and propels the solutions through the analytical manifold. A new motor was integrated that has similar operating characteristics but a slightly different physical form factor. This change in dimensions required a reengineering of the mating between the brushless dc motor and the gearing for the pump-head. The multi-position, standards-valve controller for the sensor's flow-injection analytical system also failed and required replacement. During this process it was found that the transistors that drive the motor would overheat and fail if the pressure compensated housing was not filled with the fluid that had acted as a heat sink. Eliminating the need for the pressure compensating fluid is highly desirable because it would decrease the overall weight of the sensor by approximately thirty pounds and simplify the trim and buoyancy of the final sensor packaging. A re-design of the motor controller circuit allowed the motor to operate without being submersed in a fluid to cool it. In addition, software modifications were necessary to integrate the original AUV GUI control software with the data display and analysis GUI developed for the high sensitivity laboratory version of the sensor (Masserini and Fanning, 2000). Further work focused on replacing and updating modules in the pressure-compensated portion of the system that houses the flow-injection valves and pump motor. Figure 5 presents the new framework of our nutrient sensor for AUV integration and future *in situ* testing. Components inside of the pressure compensated pump/valve housing (located on the left hand side of the figure) were upgraded.

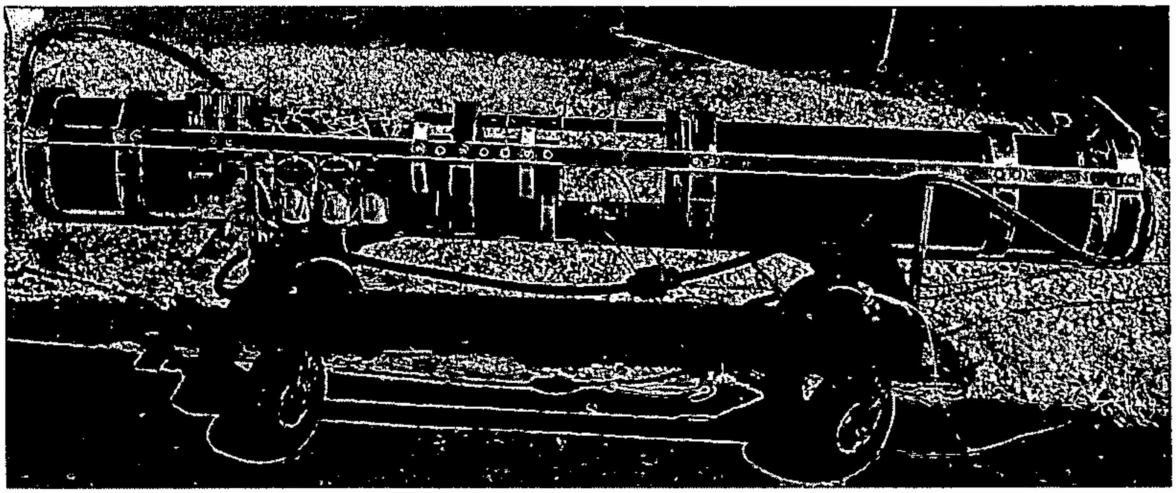

Figure 5. Bluefin AUV version of the Masserini-Fanning high sensitivity nitrogen nutrient analyzer. The pressure compensated housing for the valves and pump motor are on the left hand side of the picture and the main electronics housing is on the right hand side. The reagent reservoirs and analytical manifold are situated between the two pressure vessels.

AUV Sensor Integration

The first potential collaborator that we identified was SRI International next door to our laboratory. SRI has a Bluefin 3000 AUV, and their personnel were willing to investigate whether or not it could provide the propulsion unit we need. Unfortunately, their Bluefin did not appear capable of mating with or providing propulsion for the AUV version of our nutrient sensor, which is too large and too heavy for the Bluefin cargo design specifications. The second potential collaborator that we found who was interested in providing an AUV in which the AUV version of our nutrient sensor would occupy the cargo space was Dr. Edgar An from Florida Atlantic University's department of Engineering and Computer Science. Dr An was willing to collaborate with us in that instrumental integration, and FAU has several AUVs that might work. The fact that we have identified both a source of AUVs for the *in situ* version of our nutrient sensor and a collaborating engineer (Dr. An) bodes well that in future research we can achieve our main goal: an AUV-transported, high-sensitivity sensor for nitrate, nitrite, and ammonium in seawater. **It is of note that our underwater analyzer appears to be the only one capable of simultaneously measuring nanomolar concentrations of ammonium, nitrate, and nitrite *in situ* in the upper 300 m of the ocean. The fact that we have identified an AUV and a collaborating engineer (Dr. An of FAU) indicates that, in future research, we should be able to achieve our main goal: an AUV-transported, high-sensitivity sensor for nitrate, nitrite, and ammonium in seawater.**

A Compact Pulsed Xenon Fluorescence Analyzer for Simultaneous Detection of Nanomolar Concentrations of Nitrite, Nitrate, and Ammonium in Seawater

Another focus of this particular grant was to construct a compact lightweight version of the Masserini/Fanning (2000) sensor that can operate from smaller, less expensive research vessels. As mentioned above, use of this version, by itself or in conjunction with an AUV version, will permit much more frequent and detailed monitoring of low-level nutrient spikes in coastal waters.

In order to streamline the sensor and decrease its footprint and weight, updated designs of both the fluidic control system and the electronics components were necessary. The new system operates on 120 volt AC power instead of 24 volt DC power and can thus readily function on the standard power on board a small vessel. This cheaper, smaller, lightweight version of the "standard" operational laboratory Masserini/Fanning nutrient sensor was completed at a component cost of ~$30,000 (vs. $100,000 for the Masserini & Fanning (2000) version). Figure 6 presents the new version which is much smaller (6,800 in^3 vs. 65,000 in^3) and lighter (100 lb vs. 350 lb) than the old version and should function nicely on the *R/V Fishawk,* a vessel the size of a small charter fishing boat and costing ~$2,000 per day (vs. $9,000 per day for the *Weatherbird II*).

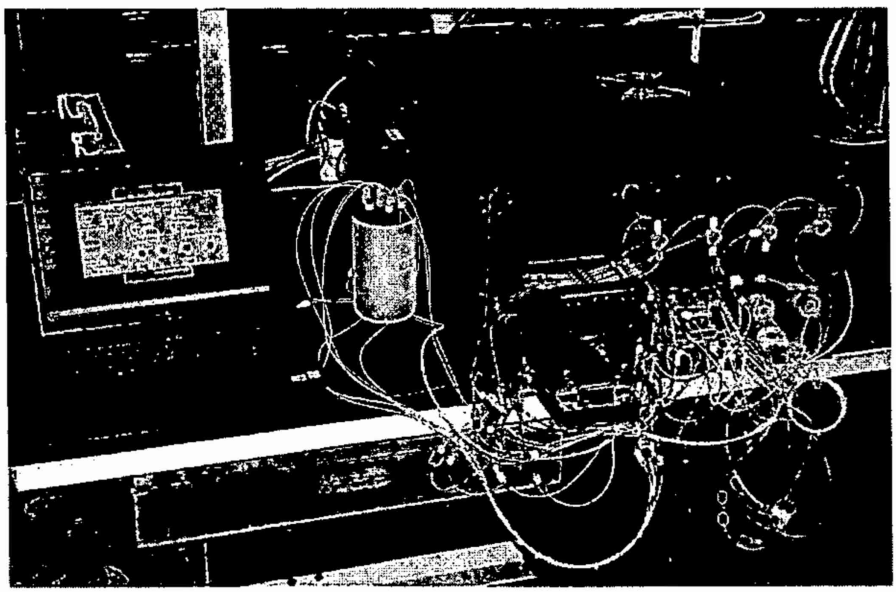

Fig. 6 The new field version of the Masserini-Fanning high sensitivity nitrogen nutrient sensor.

Figure 7 presents the block diagram of the new sensor. Laboratory bench tests indicate that the new version of the nutrient sensor has the same stability and sensitivity as the standard version for two reasons: (1) it uses the proven technology of the AUV version of the sensor and (2) adequate cooling was provided in the form of aluminum heat sinks in the framework and a fan. Whenever possible as the new version was built, upgrades of individual components (12-channel pump, circuit boards, relay controllers, etc.) were installed, to increase stability and sensitivity

even further. Typical strip charts from calibration runs and the regression data from these runs is presented in Fig. 8 and 9, respectively.

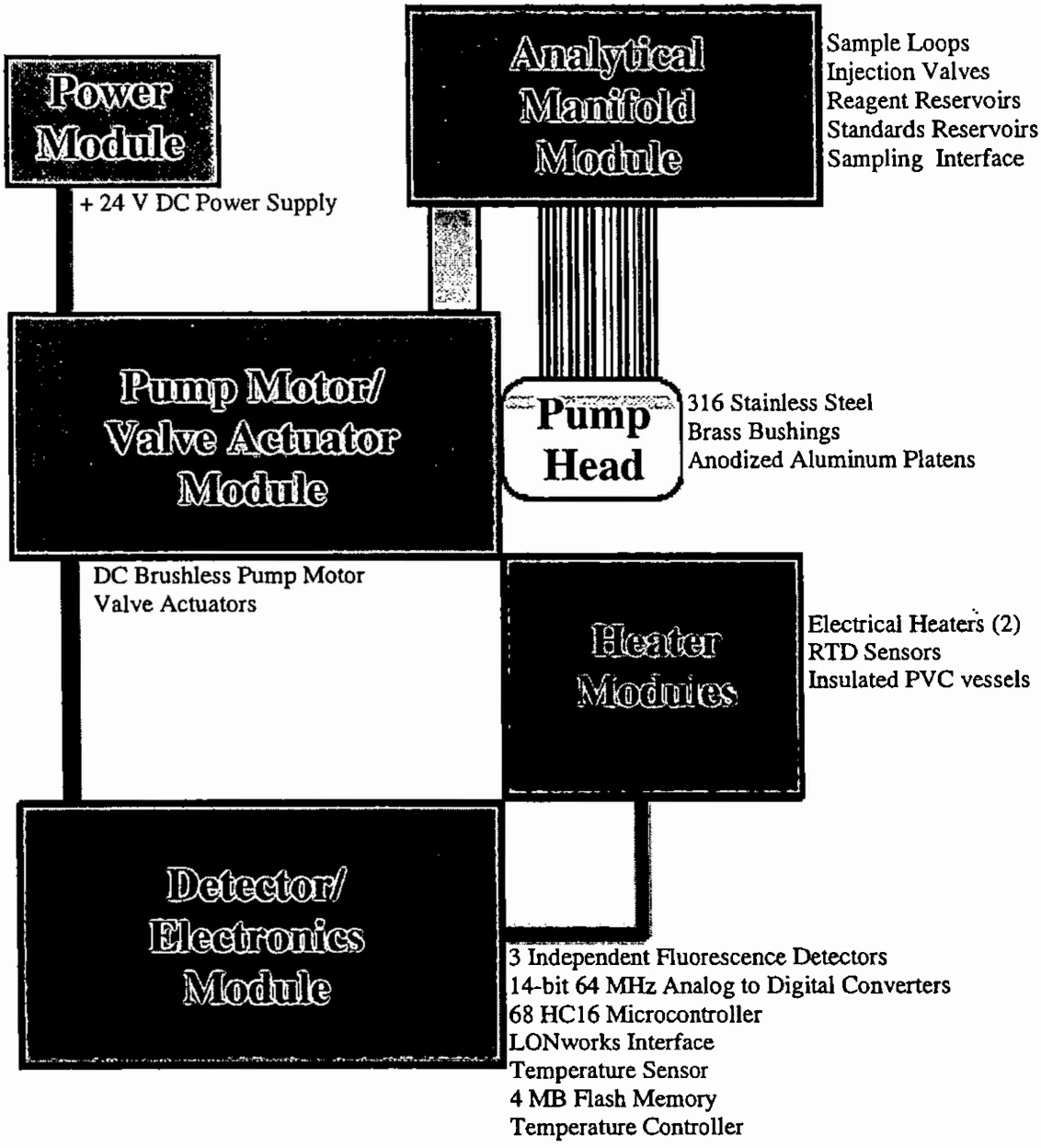

Fig. 7. Block diagram of the compact fluorescent nitrogen nutrient sensor.

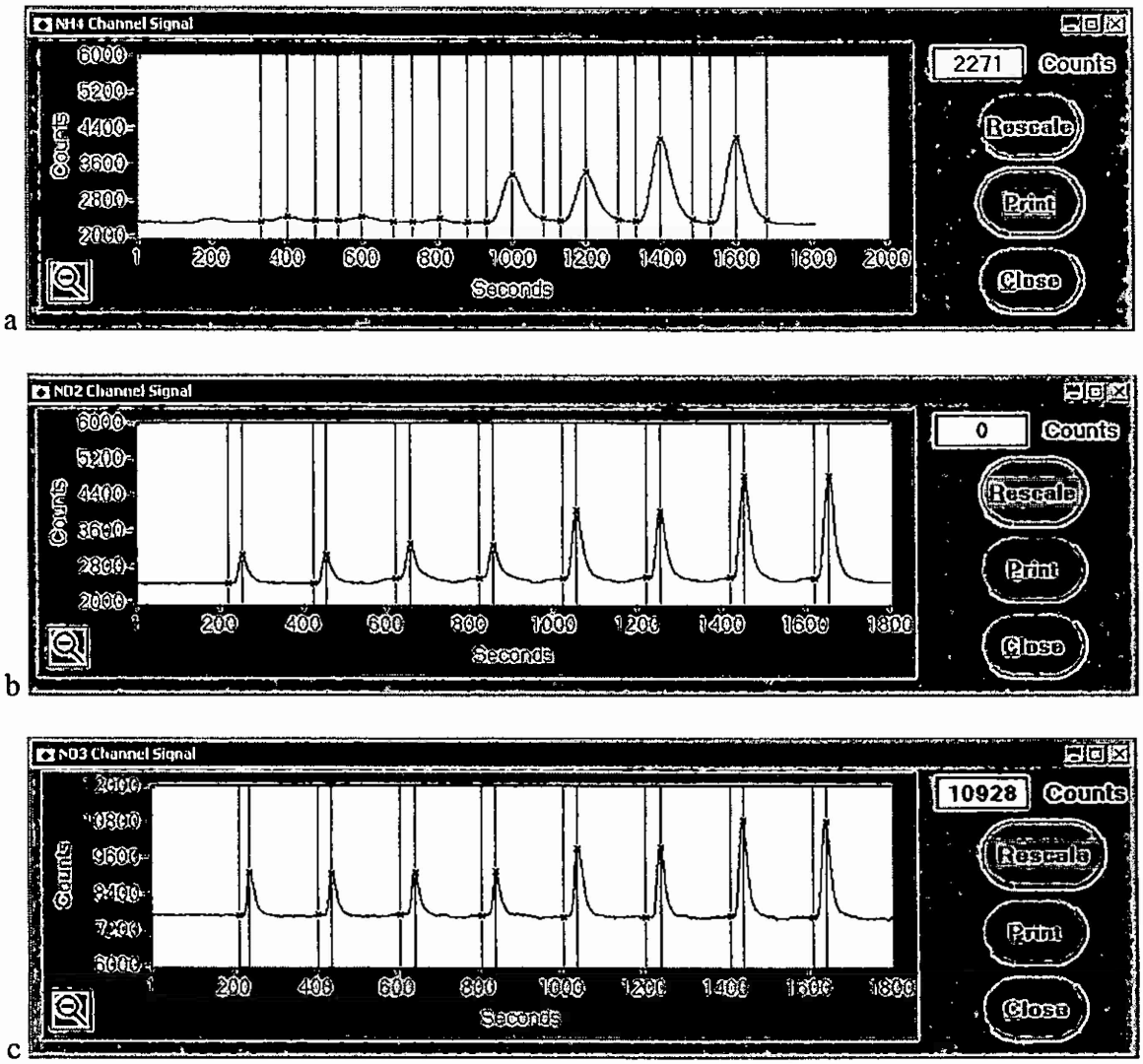

Fig. 8 Peak records for fluorescent ammonium (a), nitrite (b), and nitrate+nitrite (c) calibration standards. The first two peaks in the records are reagent blanks. The next six peaks are duplicates of spiked low nutrient seawater samples corresponding to 0, 500, and 1000 nM for ammonium and nitrite and 0, 1000, and 2000 nM nitrate+nitrite. Red and pink vertical lines indicate where the background or baseline fluorescence is measured for each sample and blue vertical lines are where the peak height for each sample is taken

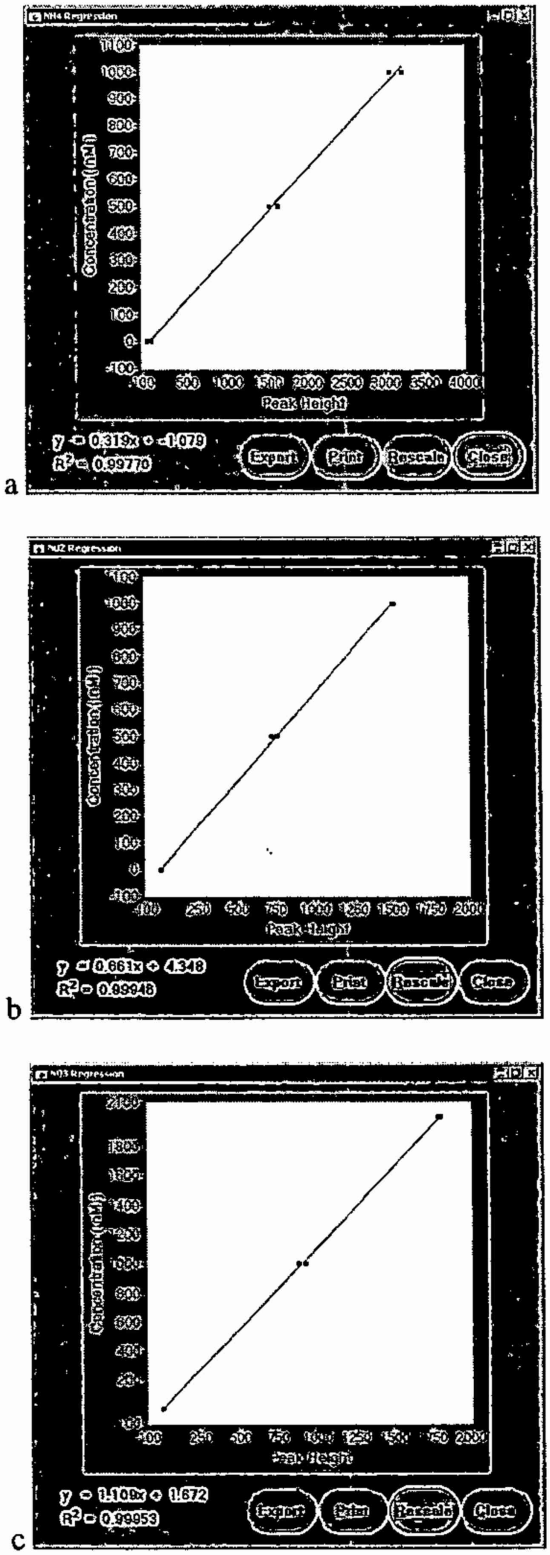

Fig. 9 Calibration curves for the fluorescent ammonium (a), nitrite (b), and nitrate+nitrite (c) calibration standards shown in Figure 8.

A two-day field test of the instrument was conducted in the summer on the *Weatherbird II* where the instrument was connected to acid-cleaned high-density polyethylene tubing married to a Vectran line and connected to a stainless-steel "fish" that was dragged behind the ship. An air-driven, chemically pure suction pump sucked seawater through the tubing up into the ship's laboratory where it was subsampled and measured for nitrate, nitrite, and ammonium. The new sensor performed up to expectations, achieving detection limits of less than 20 nM for ammonium and nitrite and less than 50 nM for nitrate. During the field test, the system detected an ammonium peak of 880 nanomolar, which contrasted sharply with most of the ammonium values, which were ~ 100 nanomolar (the "background" ammonium values found in these waters by Fanning et al., (2012)). This ammonium peak, more than twice the highest peak found before, supports the prediction made by Fanning et al. that summertime might be the best time to find ammonium peaks that might provide stronger labels or tracers for these water masses.

The sensor will play critical roles in support of remote sensing operations from fixed moorings or platforms: recalibration. Nutrient-measuring devices that are often proposed for long-term autonomous deployment on these installations present some serious difficulties. Most of the autonomous devices utilize reagents to react with nutrients, and reagents can become unstable over periods of days to months. Recalibration is thus necessary, but, unfortunately, internal nutrient recalibration standards can become unstable as well. Even if nutrient-measuring devices on fixed monitoring stations worked "perfectly," the data they generate cannot yield an adequate picture of the nutrient distribution patterns in the waters between the stations. Periodic surveys by an instrument like the "blue box" in Fig. 6 can easily provide the needed data. It can perform both calibrations and surveys on regularly scheduled transects conducted close to the installations and/or between them. The transects could be conducted via a small, cheap-to-operate vessel.

Long-Term Monitoring of Dissolved Nitrate in Ocean Water by an ISUS Ultraviolet Sensor

As mentioned under Long-Term Goals, we began the evaluation of the use of an Satlantic (now part of SeaBird Scientific) ISUS ultraviolet sensor for nitrate ion in seawater. The powerful advantage of this unit is that it uses the UV absorption by nitrate as the detection technique and thus requires no internal standards, reagents, or blank solutions that can degrade over time and make the results uncertain. A disadvantage, however, is that its detection limits (~2 μmolar) are not very sensitive for much of the upper ocean, including many coastal regions. Also the sensing unit is susceptible to biofouling. Our objective was to deploy an ISUS and ascertain its analytical and monitoring capabilities. The approach for this objective centered on maintaining the sensor array installed on the Hillsborough River as well as collecting discrete water samples to evaluate the accuracy and response of the ISUS UV nitrate sensor. Real time ISUS data are telemetered and displayed at http://comps.marine.usf.edu/index?view=station&id=UTP. Figure 10 presents the nitrate time course from the Hillsborough River station in Tampa Bay for the first half of 2009. For the first two months that ISUS #161 was deployed, its data were in reasonable agreement with the discrete colorimetric nitrate analyses performed on a Technicon AAII autoanalyzer. Later in the year ISUS #161 was replaced by another ISUS (#075), and a significant difference was found between the discrete samples and the ISUS-derived concentrations. This shift was related to an instrumental calibration offset. We have found that

the contribution from dissolved organic matter (DOM) to the UV absorption measured by the ISUS causes its nitrate values to be overestimates of the actual nitrate concentrations. Since 2009, we have continued this ISUS evaluation, including work on a means of calibrating the ISUS using standard nitrate additions to water with high DOM in order to correct for this offset. We have not found out how to make the ISUS work well for the monitoring purposes we

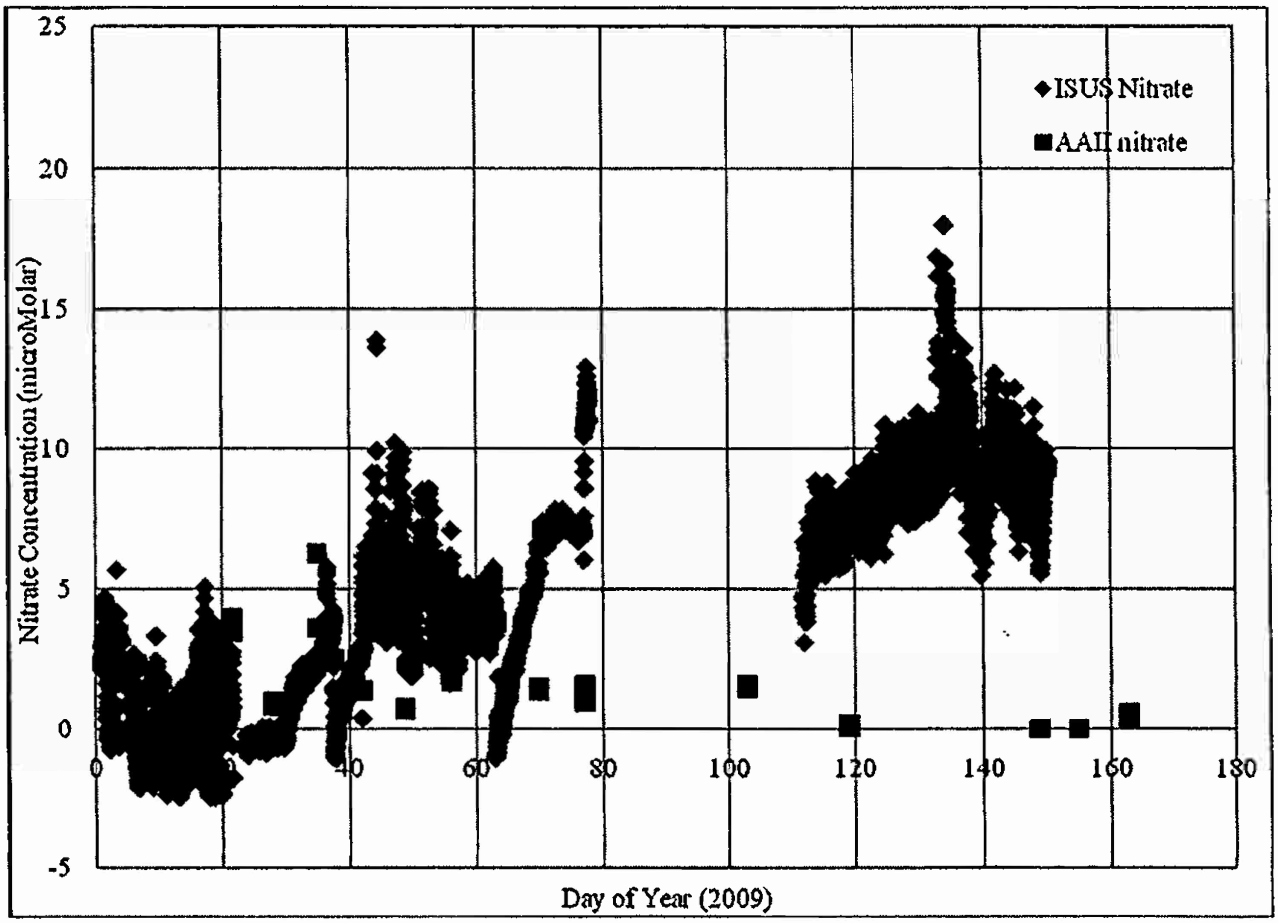

Figure 10. Nitrate time course measured at the Hillsborough River installation for the first half of 2009. Blue data points are ISUS-derived nitrate concentration, and red data points are discrete water sample nitrate values used to evaluate the ISUS response. After approximately three months the first ISUS deployed failed, and a second unit was deployed on day 111. This unit had a higher offset due to an internal calibration error.

intended. Internal component failure (like the shutter controlling the signal) happen too frequently. Biofouling is a constant problem. Data acquisition via the Web is sometimes erratic. But, we have at times seen some intersting nitrate signals which were coherent in time with reasonably smooth trends that matched salinity or other variables. So we continue with this field analytical monitoring research.

References

Dortch, Q. 1990. The interaction between ammonium and nitrate uptake in phytoplankton. *Marine Ecol. Prog. Ser.* **61**, 183-201.

Fanning, K.A., R. Masserini, J.J. Walsh, R. Wanninkhof, K. Sullivan, and J.I. Virmani. 2012. Wind forcing, ammonium events, and the nutrient regime in the surface ocean, (to be submitted)

Gordon, L.I., Jennings, J.C. Jr., Ross, A.A., and Krest, J.M. 1993. A suggested protocol for continuous flow automated analysis of seawater nutrients (phosphate, nitrate, nitrite and silicic acid in the WOCE Hydrographic Program and the Joint Global Ocean Fluxes Study. In: WOCE Hydrographic Program Office, Methods Manual WHPO 90-1

Hildebrand, M. 2005. Cloning and functional characterization of ammonium transporters from the marine diatom cylindrotheca fusiformis (bacillariophyceae). *J. Phenol.* **41**, 105-113.

Johnson, M. T., P. S. Liss, T. G. Bell, T. J. Lesworth, A. R. Baker, A. J. Hind, T. D. Jickells, K. F. Biswas, E. M. S. Woodward, and S. W. Gibb. 2008. Field observations of the ocean-atmosphere exchange of ammonia: fundamental importance of temperature as revealed by a comparison of high and low latitudes, *Global Biogeochem. Cycles.* **22**, GB1019, doi:10.1029/2007GB00309

Masserini, R. T. and K. A. Fanning. 2000. A sensor package for the simultaneous determination of nanomolar concentrations of nitrite, nitrate, and ammonia in seawater by fluorescence detection. *Mar. Chem.* **68**, 323-333.

Martin, A. P. 2003. Phytoplankton patchiness, the role of lateral stirring and mixing. *Prog. in Oceanog.* **57**, 125-174.

Mulholland, M. R., P. W. Bernhardt, C. A. Heil, D. A. Bronk, and J. M. O'Neil. 2006. Nitrogen fixation and release of fixed nitrogen by *Trichodesmium* spp. in the Gulf of Mexico. *Limnol. Oceanog.* **51**, 1762-1776.

Neumann, G and W.J. Pierson. 1966. *Principles of Physical Oceanography* (Prentice-Hall, Inc., Englewood Cliffs, NJ.

Solorzano, L. and J. H. Sharp. 1980. Determination of total dissolved nitrogen in natural waters. *Limnol. Oceanogr.* **25**, 751-754.

Valderama, J .C. 1981. The simultaneous analysis of total nitrogen and total phosphorus in natural waters. *Mar. Chem.* **10**, 109-122.

Vecchi, G. A. and B. J. Soden. 2007. Increased tropical Atlantic wind shear in model projections of global warming. *Geophys. Res. Lett.* **34**, L08702, doi:10.1029/2006GL028905

Virmani, J. I. and R. H. Weisberg. 2005. Relative humidity over the West Florida Continental shelf. *Monthly Weath. Rev.* **133**, 1671-1686.

Wanninkhof, R. 1992. Relationship between wind speed and gas exchange over the ocean. *J. Geophys. Res.* **97**, 7373-7382.

Weisberg, R. H., Y. Liu, and D. A. Mayer. 2009. West Florida Shelf mean circulation observed with long-term moorings. *Geophys. Res. Lett,* **36**, doi:10.1029/2009GL040028.

Yool, A., A. P. Martin, C. Fernández, and D. R. Clark. 2007. The significance of nitrification for oceanic new production. *Nature* **447**, 999-1002 doi:10.1038/nature 05885

Final Technical Report:

An AUV-Based Investigation Of The Role Of Nutrient Variability In The Predictive Modeling Of Physical Processes In The Littoral Ocean

Grant Number: N00014-07-1-0800

Principal Investigators:

Dr. Kent A. Fanning
College of Marine Science
University of South Florida
St. Petersburg, FL 33701
phone: (727) 553-1594
email: kaf@marine.usf.edu

Dr. Robt. T. Masserini, Jr.
College of Marine Science
University of South Florida
St. Petersburg, FL 33701
phone: (727) 553-1646
email:masserin@marine.usf.edu

Long-term Goals:

Our long-term goal is to evaluate the utility of low-level concentrations of nitrate, nitrite, and ammonium as tracers of physical processes in oligotrophic coastal waters and as descriptors of geophysical fields. To facilitate this goal, a primary focus has been adapting our laboratory sensor for use in an autonomous underwater vehicle (AUV). In addition to further work on an AUV version, a new focus for this grant was to construct a compact lightweight version of the Masserini/Fanning (2000) sensor that can operate from smaller and cheaper research vessels. Use of this version, by itself or in conjunction with an AUV version, will permit much more frequent and detailed monitoring of low-level nutrient spikes in coastal waters. The utility of tiny increases in nitrogenous nutrients for detecting manmade benthic disturbances in coastal waters is an important component of our research since these increases can also be tracers.

Biological processes produce variations in nutrient concentrations throughout the ocean. Usually, the biggest differences in nutrient concentrations occur between surface water and deep water or between one mass of deep water and another mass of deep water. These differences have been utilized for some time to identify and track deep-water masses, but the surface ocean is different. Surface nutrient concentrations in most of the oceans tend to be low, so low in fact that the standard nutrient techniques (e.g., Gordon et al., 1993) have detection limits that are approximately the same magnitudes as the concentrations, thus precluding the detection of surface-water concentration differences. However, we developed a high-sensitivity fluorescent sensor for three of those nutrients (nitrate, nitrite, and ammonium) that had detection limits considerably lower than their surface nutrient concentrations (Masserini and Fanning, 2000). This sensor offers the exciting prospect of using these nutrients as "tags" for masses of surface water that will track those masses when conventional measures like temperature and salinity might not. Further, a miniaturized Masserini-Fanning sensor operating independently in an AUV to obtain *in situ* nutrient measurements could thus evaluate the horizontal sizes and distributions of surface seawater masses through simultaneous mapping efforts with the shipboard version of

the Masserini-Fanning sensor. The AUV version would also permit much greater coverage of nutrient-enriched boluses in deeper layers within the surface ocean, which can now only be studied by the much less definitive process of CTD rosette hydrocasts.

We also began to evaluate the feasibility of using ISUS ultraviolet *in situ* sensors in long-term monitoring of nitrate inputs to coastal waters and nitrate pulses near shore.

This report presents our progress toward these long-term goals.

Lagrangian Experiments On Surface Ammonium Events

Two Lagrangian experiments on ammonium (NH_4^+) were conducted using sulfur hexafluoride to label surface water masses. The site of the experiments (FSLE V and FSLE VI) was the low-nutrient euphotic zone in continental-margin waters of the eastern Gulf of Mexico (Fig. 1). The biogeochemical cycling of nitrate, nitrite, and ammonium were monitored within the labeled regions over the course of the experiments. The methodology, experimental details, and results previously reported in the Final Technical report for grant N00014-02-1-0240 are summarized here, followed by the more recent data analysis conducted under this grant. The resultant wind speed, barometric pressure, and ammonium data for FSLE V and VI are presented in Figures 2 and 3, respectively.

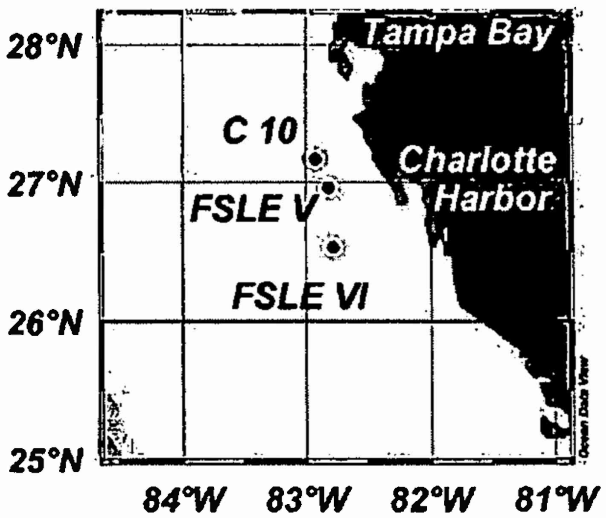

Fig. 1. Locations of SF_6 injection sites for the FSLE V and FSLE VI experiments in the eastern Gulf of Mexico in April, 2001 and November, 2002, respectively. The SF_6-labeled surface seawater tended to drift southward during the experiments, in accord with the general circulation patterns (Weisberg et al. 2009). The location of a nearby current-meter mooring with meteorological instrumentation (C10) is also shown; C10 is part of the West Florida Shelf mooring array maintained by the University of South Florida COMPS program (http://comps.marine.usf.edu/

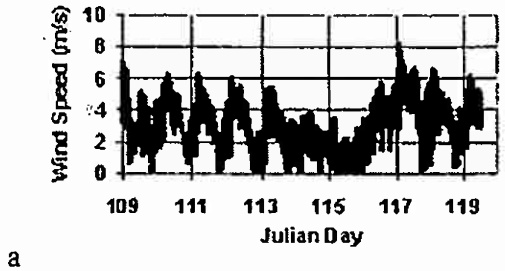

a

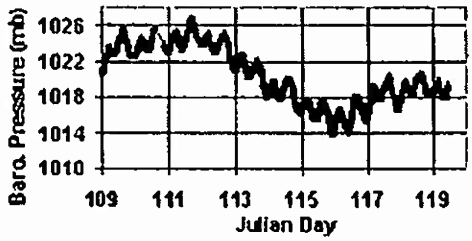

b

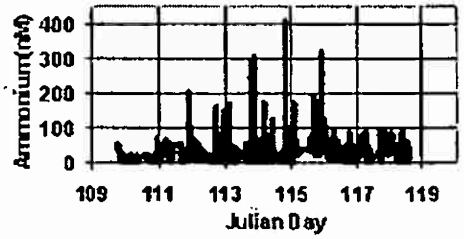

c

Fig. 2. Time courses of wind speed (a), barometric pressure (b), and NH_4^+ concentration (c) in the upper 2 meters of the ocean during the FSLE V experiment on the West Florida continental shelf between Julian Days 110 and 118.5 in April, 2001. Wind speeds, measured by an anemometer on the research vessel (F.G. Walton Smith) and corrected for ship's speed and direction, agree with the regional patterns from measurements on COMPS mooring C10 (Fig. 1). NH_4^+ concentrations, measured on seawater flowing into the dedicated seawater system of the research vessel, show the presence of maxima as "peaks" above background NH_4^+ concentrations (0-80 nmol L^{-1}).

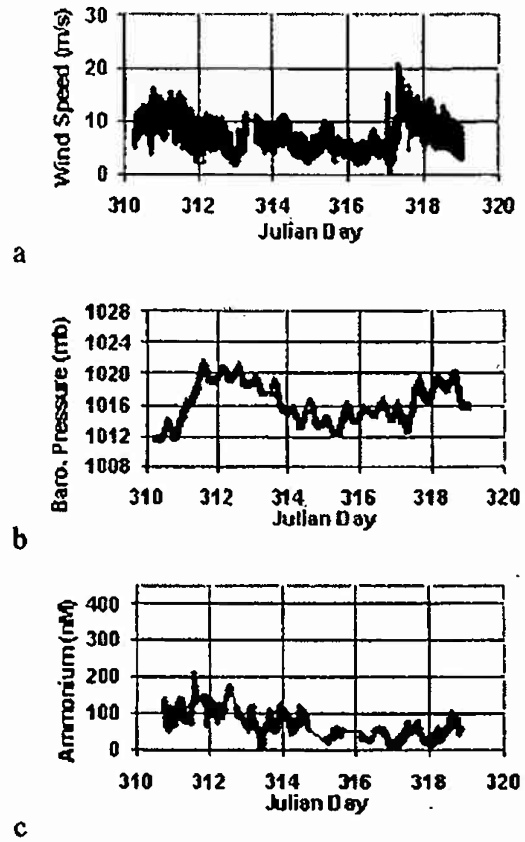

Fig. 3. Time course of wind speed (a), barometric pressure (b), and NH_4^+ concentration (c) in the upper 2 meters of the ocean during the FSLE VI experiment on the West Florida continental Shelf between Julian Day 310.5 and 319 in November, 2002. Wind speeds, measured by an anemometer on the research vessel (F.G. Walton Smith) and corrected for ship's speed and direction, agree with the regional patterns from measurements on COMPS mooring C10 (Fig. 1). NH_4^+ concentrations, measured on seawater flowing into the dedicated seawater system of the research vessel, show the presence of maxima as "peaks" above background NH_4^+ concentrations (0-80 nmol L^{-1}).

The principal observations of our two-experiment field study were the ammonium event (= a clustering of enriched ammonium concentration peaks) during FSLE V and the lack of an ammonium event during FSLE VI. Unfortunately though, the patterns of several commonly measured environmental parameters in the water column provided little help in explaining either one. Salinity ranges were nearly identical: FSLE V (36.37-36.56) vs. FSLE VI (36.28-36.39), as were fluorometric chlorophyll values: FSLE V (0.08-0.60 $\mu g\ l^{-1}$) vs. FSLE VI (0.07-0.41 $\mu g\ l^{-1}$). Temperatures on FSLE VI (26.32-27.42°C) were warmer than on FSLE V (19.62-22.70°C), but this difference was most likely unimportant.

The only other available environmental parameters in FSLE V and FSLE VI were meteorological, and examination of the time courses of wind speed and barometric pressure suggested a plausible explanation of the ammonium features and trends in both experiments. During FSLE V, variations in meteorological parameters, as measured on shipboard (Fig. 2a and

b) and confirmed for the study region by instruments on mooring C10 (Fig. 1), appeared to coincide with the presence or absence of [NH_4^+] maxima (Fig. 2c). From JD 110 through part of JD 111, wind speeds were mostly ~1 ms^{-1} to ~7 ms^{-1}, while barometric pressure was 1022-1027 mb. But, near the end of JD 111, both parameters began to change. Wind speeds decreased, with minimum values becoming ≤1 ms^{-1} for increasingly long periods of time and maximum wind speeds declining, eventually to ≤4 ms^{-1} at JD 114 – 116. Barometric pressure decreased to 1014 -1019 mb. Then both wind speed and barometric pressure increased rather sharply, mostly during JD 116. These wind-speed and barometric-pressure patterns indicate the approach and passage of a low-pressure weather front (Virmani and Weisberg 2005). The period of calming winds ahead of the front was of particular interest because it coincided so closely with the period in which the strong [NH_4^+] maxima were present -- i.e., the ammonium event in Fig. 2c during JD 112-116. When wind speeds and barometric pressure subsequently increased during frontal passage on JD 116, the maxima, and the event, disappeared.

Winds generate sea-surface wind stress, enhancing turbulence. The natural clumping of planktonic organisms into patches is well known (Martin 2003), and ammonium concentrations should be higher in patches abundant with bacteria and other organisms responsible for ammonium release during organic-matter remineralization. Faster wind speeds lead to greater wind stress and should produce more intense mixing between such patches and the surrounding seawater, resulting in the dispersion of the organisms and the dilution of the ammonium concentrations.

Once wind speeds weaken -- for example preceding an approaching low-pressure front -- mixing should also weaken, and the concentrations of the remineralization-producing organisms and the NH_4^+ they release would be expected to increase within patches. Each FSLE V [NH_4^+] maximum in the ammonium event (Fig. 2c) appeared as a coherent bolus or "patch" with a peak in concentration . Distances across these peaks, estimated from the positions of the beginnings and endings of the peaks, were 1.1-4.4 km, or in the low end of the mesoscale/sub-mesoscale range (1-100 km) that describes features like filaments, eddies, etc. customarily considered as patches (Martin 2003).

Wind behavior can also explain the disparity between FSLE V results and FSLE VI results, even though a preliminary examination of Fig. 3 (a and b) suggests that the weather pattern of FSLE VI in fact resembled that of FSLE V. The decline of wind speed and barometric pressure between JD 311.5 and JD 317, followed by strong increases in both parameters, clearly denotes the approach and passage of a weather front (Virmani and Weisberg 2005) during FSLE VI, just as seen in FSLE V -- Fig. 2 (a and b). FSLE VI might thus have been expected to exhibit an ammonium event with [NH_4^+] maxima ≈400 nmol L^{-1}. However, closer examination reveals a fundamental difference: FSLE VI wind speeds were considerably higher than FSLE V wind speeds. (Notice the difference between the wind-speed scales in Figs. 2a and 3a). FSLE V wind speeds frequently dropped to zero, especially during JD 114-116, when the ammonium peaks were particularly strong (Fig. 2c), and were never above 8.2 ms^{-1}. In contrast, FSLE VI wind speeds were often >10 ms^{-1}, and even reached 15-22 ms^{-1} (Fig. 3a).

The differing effects of wind in FSLE V and FSLE VI are highlighted by two types of analysis: average daily wind speeds and dispersion estimates.

Calculations on wind data from the *RV F.G. Walton Smith* demonstrated the different potential impacts of wind speed during FSLE V and FSLE VI (Table 1). The approach was to calculate time patterns in wind speed for each experiment, beginning even before the first instances (called time zero in Table 1) when loci of maxima in SF_6 concentration were first identified within the SF_6-labeled areas of seawater. The average daily wind speed was calculated for a 12-day period in FSLE V and a 9-day period in FSLE VI. The much greater wind impact in FSLE VI is clearly evident. During FSLE V, the highest average daily wind speed was 6.3 ms^{-1}, and all but two of the average daily wind speeds in FSLE VI are larger than that. The lowest average daily FSLE V wind speeds of ~1 ms^{-1} occurred on JD 114-115, during the calm period before frontal passage, and were coincident with the ammonium event (Fig. 2c). In contrast, the approximately five-fold higher lowest average daily FSLE VI wind speeds occurred on JD 315-317, during the calm period before frontal passage, and were coincident with ammonium concentrations that were essentially at background levels (Fig. 3c).

Table 1. *Average daily wind speeds calculated from shipboard, motion-corrected anemometer data on R/V F. G. Walton Smith during the FSLE V and FSLE VI experiments. Time values from Fig. 2 (a-c) and Fig. 3 (a-c) are presented for comparison, and the corresponding Julian days are also presented.*

FSLE V			FSLE VI		
Julian Day	Time in Fig. 2 (d)	Average daily wind speed (ms^{-1})	Julian Day	Time in Fig. 3 (d)	Average daily wind speed (ms^{-1})
108		6.3	310		10.2
109		2.8	311		8.9
110	0	3.8	312	0	6.7
111	1	3.1	313	1	6.7
112	2	3.1	314	2	6.4
113	3	2.7	315	3	5.9
114	4	1.9	316	4	4.8
115	5	0.9	317	5	9.2
116	6	3.5	318	6	8.0
117	7	4.6			
118	8	3.5			
119	9	4.1			

The interactions of wind with the sea surface, which are important for dispersion processes as well as gas exchange with the atmosphere, can be quite sensitive to differences in wind forcing, such as presented in Table 1. Sea-surface wind stress (a parameter related to frictional effects of wind on these processes) typically varies with the magnitude of the wind speed raised to a power on the order of two (Neumann and Pierson 1966). After SF_6 injection into a seawater parcel, SF_6 concentration will decline because of atmospheric gas exchange and because the water parcel disperses into its surroundings and mixes with those waters, in which the SF_6 concentration is zero. This dispersion and mixing will also tend to reduce any maximum in $[NH_4^+]$ because $[NH_4^+]$ is lower in the seawater surrounding the maximum. SF_6 can thus serve as a "proxy" for NH_4^+ in evaluating the effects of dispersion and mixing, once corrections for SF_6 gas exchange are applied.

Wind forcing enters this exchange evaluation as the square of the wind speed when the SF_6 gas exchange coefficient (k) is calculated using coefficients derived from the gas transfer of oxides of stable carbon and radiocarbon (Wanninkhof 1992). The net air-sea SF_6 gas exchange flux (F) is proportional to the difference between the concentration of SF_6 in the seawater (C_w) and the

concentration of SF_6 in air (C_a). But, since C_a may be assumed to be zero, $F = k \bullet C_w$, which makes the flux a first-order process. Consider a volume of seawater (V) of area "A" and average depth "h" in the ocean's mixed layer. Now $V = A \bullet h$; so the total mass of SF_6 gas in the seawater is $M = V \bullet C_w = A \bullet h \bullet C_w$. The net flux F of SF_6 across the air-sea interface -- in mass/unit area/unit time (t) -- is then given by:

$$F = (A)^{-1} \bullet dM/dt = h \bullet dC_w/dt = k\,(C_w),$$

where C_w = the concentration of SF_6 remaining in the seawater at time = t, and dC_w/dt = rate of decline in SF_6 concentration in the mixed layer volume V due to loss to the atmosphere. Integration of "$h \bullet dC_w/dt = k\,(C_w)$" yields:

$$C_w/C_{wo} = \exp\,(k \bullet h^{-1} \bullet t) = f_{exch} \qquad \text{(Eq. 1)},$$

where $C_w/C_{wo} = f_{exch}$ represents the fraction of the original SF_6 concentration (C_{wo} at time = 0) remaining in seawater volume V after gas exchange has occurred for a time period = t.
Of course, dispersion has occurred during the same time period, and thus the fraction of the original concentration of SF_6 remaining after gas exchange (f_{exch}) has been reduced further by another fraction that represents the effect of dispersion: f_{disp}. The actual measured value of C_w is significantly less than the C_w value that would be present if only gas exchange were occurring, and the actual measured fraction of the original concentration of SF_6 that remains after time t (f_{total}) is given by: $f_{total} = f_{exch} \bullet f_{disp}$. This equation may be rearranged to solve for f_{disp} as follows:

$$f_{disp} = f_{exch} \bullet (f_{total})^{-1} \qquad \text{(Eq. 2)}$$

As discussed below when presenting the work of Johnson et al. (2008), ammonium need not be assumed to undergo a significant gas-exchange process with the atmosphere at the time scales considered here. So the only physical process that could reduce ammonium concentration may be assumed to be dispersion, and values for f_{disp} obtained for SF_6 would also apply to any solute, e.g., ammonium. The measure of the impact of the dispersion that affected ammonium concentrations in surface waters during the FSLE V and FSLE VI experiments was obtained from the changes in the SF_6 concentration present at different times after time zero. Once time zero was selected for each experiment, the values of f_{exch} at different times (t) were calculated from Eq. (1), where k was obtained from Eq. (3) of Wanninkhof (1992) utilizing wind-speed data from the *R/V F.G. Walton Smith*. The average water depth (h) in Eq. 1 was taken to be 25 m. The field protocol on both experiments was to survey the SF_6-labeled regions of surface water in a manner that could identify the loci of maximum SF_6 concentrations within them at the values of "t" that corresponded to calculated values of f_{exch}. These loci identified the approximate centers of the dispersing SF_6, with time zero in each experiment being established when the first sampling of the center of the labeled area occurred. Division of these maximum concentrations by the initial SF_6 concentrations in the centers of the labeled areas at time zero yielded the values of f_{total} corresponding to the f_{exch} values, and Eq (2) was then used to calculate the values of f_{disp} that described the dispersion of ammonium ions in the labeled areas during FSLE V and FSLE VI.
A comparison of the temporal trends of ln f_{disp} against time (Fig. 4) indicated that dispersion was distinctly different in the two experiments. The magnitude of the negative slope of ln f_{disp} vs

time was 68% larger for FSLE VI than for FSLE V. Thus, after 3 days, the fraction of SF_6 remaining in the center of the FSLE V labeled area was ~2 times greater than in the FSLE VI labeled area. After 6 days the fraction of SF_6 remaining in the center of the FSLE V labeled area was ~4 times greater than in the FSLE VI labeled area. These estimates indicate a much greater

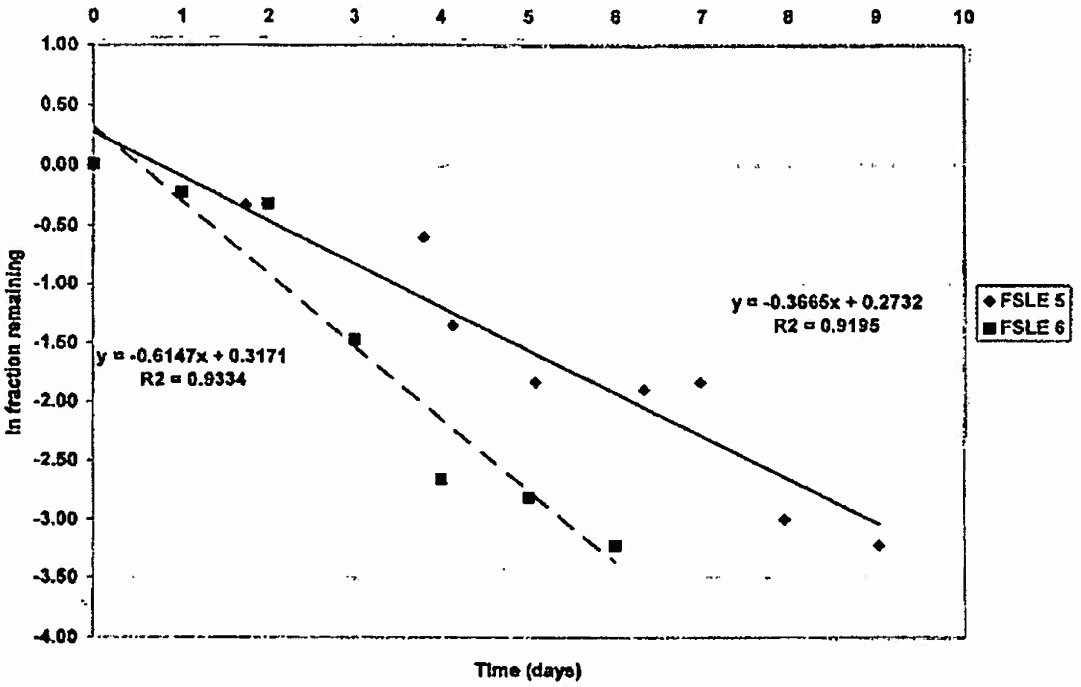

Fig. 4. The time variation of the natural logarithm of the mass fraction of SF_6 (f_{disp}) remaining in the centers of the SF_6-labeled areas of coastal water during the FSLE V and FSLE VI experiments after correction for SF_6 loss due to gas exchanges with the atmosphere. f_{disp} is also a measure of the relative reduction in ammonium concentrations as a result of dispersion (mixing) processes during FSLE V and VI (see text).

dispersion for the FSLE VI experiment, affecting both SF_6 and ammonium concentrations. Overall then, wind-regime comparisons indicated that average daily wind speeds were up to 10-fold higher and wind-driven dispersion of ammonium was accordingly 2-4 times higher in FSLE VI than in FSLE V.

The duration of the FSLE V ammonium maxima and the possible sources of the ammonium that formed the maxima are also important aspects to consider.

Under many circumstances, marine phytoplankton prefer ammonium over nitrate as a nitrogen source (Dortch 1990). Utilization of ammonium requires less energy since its nitrogen is fully reduced and is an immediate precursor to amino-acid nitrogen. Nitrate, by contrast, requires reduction by eight electrons per ion in order to be as usable (Hildebrand 2005). So an obvious question to ask is, "Given that ammonium is such a critical nutrient, should we not have expected the phytoplankton in Gulf of Mexico surface waters in the FSLE V experiment to consume any remineralized ammonium as fast as it appeared, with the result that duration times of ammonium

concentration maxima or "peaks" would be effectively zero?" As part of a study of *Trichodesmium* species, ammonium uptake rates by phytoplankton were measured in those waters during 2001-2002 – see Table 6 of Mulholland et al. (2006). These rates can be used to estimate the duration times of the FSLE V ammonium maxima and thus address the question. The Mulholland et al (2006) uptake rates ranged from 6 to 67 nmol L^{-1} /hr when the red-tide organism *K. brevis* was absent (as was true during FSLE V). The largest FSLE V ammonium maximum was 434 nmol L^{-1}, or 354 nmol L^{-1} above the highest observed background concentration: 80 nmol L^{-1}. Thus, if we ignore any ammonium production that may have occurred during the sampling transect across that maximum, it would have been reduced to background in t = 354 nmol L^{-1} /(6 to 67 nmol L^{-1}/hr) = 5.3 to 59 hr. Similarly, a FSLE V ammonium maximum of 200 nmol L^{-1} is 120 nmol L^{-1} above the same background and would have been reduced to background in t = 1.8 to 20 hr. These ranges provide estimates of the duration times of the ammonium maxima in FSLE V, but are most likely underestimates since ammonium production was ignored.

The field-sampling protocol utilizing the Masserini-Fanning system was able to transect and fully define all ammonium peaks in 0.17 to 0.97 hr. Since these transit times are much smaller than the estimated peak duration times, ammonium uptake by primary producers was not rapid enough to prevent the peaks from being detected. In fact, the longest estimated ammonium peak duration times compare favorably with the entire 4-day interval between JD 112 and JD 116 when the ammonium event occurred in FSLE V (see Fig. 2c). If we make the reasonable assumption that ammonium production was also occurring, then some of the larger peaks (i.e., ammonium enrichments) should have persisted during most of that interval. The duration times of the ammonium peaks in FSLE V were far from zero.

Another question concerns the source(s) of the ammonium in the maxima observed during FSLE V, once again keeping in mind that no red tide (i.e., *K. brevis*) was present. Within the water column, two such sources are possible: dissolved organic nitrogen (DON) and particulate organic nitrogen (PON). DON concentrations determined by the Solorzano and Sharp (1980) and Valderama (1981) methods in the same Gulf of Mexico surface waters in 2002 (when red tide was also absent) averaged 8300 ± 1200 nmol L^{-1}. Although no DON values were measured during 2001, the 2002 results matched reasonably well with later DON results for the same waters when red tide was absent in 2004: 9100 ± 500 nmol L^{-1}. So it would be reasonable to assume that the DON concentration in the FSLE V experimental area is typically ~8000 nmol L^{-1} in the absence of red tide. Next, data on PON from CHN analyses in April 2001 averaged 3250 ± 1750 nmol L^{-1}, making the estimated total concentration of DON + PON during FSLE V equal to 11,250 nmol L^{-1}. Thus an ammonium release sufficient to produce the highest observed ammonium enrichment above background during FSLE V (354 nmol L^{-1}) would have required that only 3% of the total available organic nitrogen in the water column be remineralized by ammonifying organisms.

A study of air-sea exchanges of $NH_{3(g)}$, the volatile form of total dissolved ammonia, by Johnson et al. (2008) raises the issue of these exchanges as possible atmospheric sources for dissolved ammonium in the upper ocean. The potential significance of these fluxes to the ammonium-event study may be assessed as follows. Johnson et al. (2008) estimated the magnitudes and directions of $NH_{3(g)}$ exchanges at different latitudes and temperatures in the Atlantic. They

concluded that warm ocean temperatures at latitudes of 20-30°N, such as encountered at FSLE V and VI, tended to make seawater a net *source* of $NH_{3(g)}$ to the atmosphere. This conclusion suggests that the atmosphere could not have been the source of dissolved ammonium maxima, such as found during FSLE V.

But could the upward ammonium fluxes have caused a reduction in the magnitudes of the maxima in FSLE V? A typical $NH_{3(g)}$ flux for 20-30 °N latitude is 50 pmol m^{-2} s^{-1} -- Johnson et al. (2008), Fig. 6 and Fig. 7. This rate of loss would reduce the ammonium concentration in the top cubic meter by approximately 4 nmol L^{-1} per day. However, the CTD hydrocasts conducted during FSLE V found that the thicknesses of the boluses containing ammonium enrichments during the ammonium event were on the order of 5 meters. Therefore, a more appropriate calculation would consider the top five meters of the water column. If we assume that the upward ammonium flux affects the total ammonium concentration in the upper 5 meters of the ocean, it would deplete that concentration at a rate of 10 fmol L^{-1} s^{-1}. At this rate, the sea-to-air flux of $NH_{3(g)}$ would require ~400 days to consume the 354 nmol L^{-1} maximum above background in FSLE V. If the flux were doubled, it would require ~200 days to consume the 354 nmol L^{-1} FSLE V maximum. The lifetimes of the FSLE V maxima appear to on the order of 5 days, and the magnitudes and time scales associated with measured FSLE maxima seem to have been very different from those of air-sea ammonia fluxes. Based on data available then, the magnitudes and time scales of the upward air-sea ammonium fluxes estimated by Johnson et al. (2008) would appear to be too small to have had a meaningful impact on the FSLE V ammonium maxima. This finding supports the assumption that loss of ammonium to the atmosphere is negligible when using Eq. 2 (above) to estimate the ammonium dispersion coefficient, f_{disp}.

The implication of these results relates to the mechanism of recycled primary production in the ocean, for which ammonium is a critical nutrient. The fact that weakening winds might lead to substantial relative ammonium enrichments over time periods of days suggests a mechanism whereby planktonic primary producers can, in effect, receive localized ammonium "supplements" that then stimulate photosynthesis, and carbon fixation rates, to rise above their normal magnitudes at background ammonium levels.

Wind-influenced ammonium enrichments could be rather frequent. Each year the eastern Gulf of Mexico receives on average 7-8 winter storm fronts (Virmani and Weisberg 2005) such as observed in FSLE V and VI, and 24-hour, low-pass filtered hourly wind-speed data from the nearby COMPS current mooring C10 (Fig. 1) established that wind speeds persisted below 4 ms^{-1} for two days or more 72 times in 2001, suggesting ample opportunities during a year for calming winds to permit ammonium accumulation. Sixty-four percent of these opportunities occurred in May-August, the warmer and wetter season. These results point to wind-related ammonium events as part of a mechanism for enhancing the rate of oceanic ammonium cycling. The implication is that calm winds occurring throughout the ocean from time to time may thus lead to pulses of euphotic-zone ammonium enrichments. *The estimated lifetimes of these pulses suggest that pulse features and distribution may serve as an indicator of the smaller-scale impact of wind stress in the surface ocean. Too much wind stress obliterates ammonium peaks. As wind stress weakens, ammonium peaks begin to appear and mark the areas impacted by the weakening. With further wind stress weakening, ammonium peaks grow very large and may help to identify large "patches" of surface seawater wherein organisms may be concentrated. These*

discoveries provide the rationale behind the idea of using our nutrient sensor (s) to map the horizontal distribution of surface water masses mentioned in the Long Term Goals section above.

Other ramifications of ammonium events are worth considering in view of the modeled importance of nitrification in the oceanic euphotic zone (Yool et al. 2007), the possible changes to surface wind-stress in a warming climate (Vecchi and Soden 2007), the potential importance of air-sea ammonia fluxes (Johnson et al. 2008), and the long-standing question of the principal drivers of carbon fixation in the low-nutrient, oligotrophic ocean.

Progress On Designing and Constructing an AUV Version of the Masserini/Fanning Nutrient Sensor

Under the previous grant (N00014-02-1-0240), we developed a robust submersible analyzer that would accurately elucidate the distribution of nitrate, nitrite, and ammonium within oligotrophic systems simultaneously with high resolution, both temporally and spatially, and with detection limits of less than 20 nM for all three nutrients. However that AUV version of our nutrient sensor was designed for Florida Atlantic University's Ocean Explorer (OEX) AUV, which then became unavailable to us. So we remodeled the AUV version with a form factor similar to that of the *Bluefin* AUV. The repackaging work for this objective was designed to prepare the sensor for future *in situ* testing. A modular 10.5-inch diameter framework was fabricated to hold the sensor components inside the payload cowling of a Bluefin AUV. Integration of the new sensor power system and electronics with the original pump and valve module required a significant amount of effort due to the failure of the brushless dc motor that drives the pump-head and propels the solutions through the analytical manifold. A new motor was integrated that has similar operating characteristics but a slightly different physical form factor. This change in dimensions required a reengineering of the mating between the brushless dc motor and the gearing for the pump-head. The multi-position, standards-valve controller for the sensor's flow-injection analytical system also failed and required replacement. During this process it was found that the transistors that drive the motor would overheat and fail if the pressure compensated housing was not filled with the fluid that had acted as a heat sink. Eliminating the need for the pressure compensating fluid is highly desirable because it would decrease the overall weight of the sensor by approximately thirty pounds and simplify the trim and buoyancy of the final sensor packaging. A re-design of the motor controller circuit allowed the motor to operate without being submersed in a fluid to cool it. In addition, software modifications were necessary to integrate the original AUV GUI control software with the data display and analysis GUI developed for the high sensitivity laboratory version of the sensor (Masserini and Fanning, 2000). Further work focused on replacing and updating modules in the pressure-compensated portion of the system that houses the flow-injection valves and pump motor. Figure 5 presents the new framework of our nutrient sensor for AUV integration and future *in situ* testing. Components inside of the pressure compensated pump/valve housing (located on the left hand side of the figure) were upgraded.

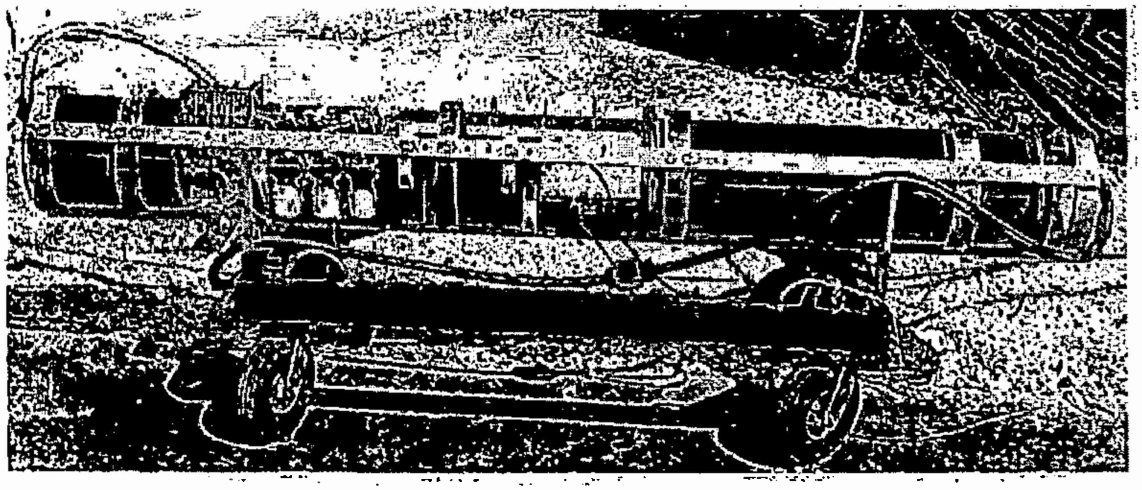

Figure 5. Bluefin AUV version of the Masserini-Fanning high sensitivity nitrogen nutrient analyzer. The pressure compensated housing for the valves and pump motor are on the left hand side of the picture and the main electronics housing is on the right hand side. The reagent reservoirs and analytical manifold are situated between the two pressure vessels.

AUV Sensor Integration

The first potential collaborator that we identified was SRI International next door to our laboratory. SRI has a Bluefin 3000 AUV, and their personnel were willing to investigate whether or not it could provide the propulsion unit we need. Unfortunately, their Bluefin did not appear capable of mating with or providing propulsion for the AUV version of our nutrient sensor, which is too large and too heavy for the Bluefin cargo design specifications. The second potential collaborator that we found who was interested in providing an AUV in which the AUV version of our nutrient sensor would occupy the cargo space was Dr. Edgar An from Florida Atlantic University's department of Engineering and Computer Science. Dr An was willing to collaborate with us in that instrumental integration, and FAU has several AUVs that might work. The fact that we have identified both a source of AUVs for the *in situ* version of our nutrient sensor and a collaborating engineer (Dr. An) bodes well that in future research we can achieve our main goal: an AUV-transported, high-sensitivity sensor for nitrate, nitrite, and ammonium in seawater. **It is of note that our underwater analyzer appears to be the only one capable of simultaneously measuring nanomolar concentrations of ammonium, nitrate, and nitrite *in situ* in the upper 300 m of the ocean. The fact that we have identified an AUV and a collaborating engineer (Dr. An of FAU) indicates that, in future research, we should be able to achieve our main goal: an AUV-transported, high-sensitivity sensor for nitrate, nitrite, and ammonium in seawater.**

A Compact Pulsed Xenon Fluorescence Analyzer for Simultaneous Detection of Nanomolar Concentrations of Nitrite, Nitrate, and Ammonium in Seawater

Another focus of this particular grant was to construct a compact lightweight version of the Masserini/Fanning (2000) sensor that can operate from smaller, less expensive research vessels. As mentioned above, use of this version, by itself or in conjunction with an AUV version, will permit much more frequent and detailed monitoring of low-level nutrient spikes in coastal waters.

In order to streamline the sensor and decrease its footprint and weight, updated designs of both the fluidic control system and the electronics components were necessary. The new system operates on 120 volt AC power instead of 24 volt DC power and can thus readily function on the standard power on board a small vessel. This cheaper, smaller, lightweight version of the "standard" operational laboratory Masserini/Fanning nutrient sensor was completed at a component cost of ~$30,000 (vs. $100,000 for the Masserini & Fanning (2000) version). Figure 6 presents the new version which is much smaller (6,800 in^3 vs. 65,000 in^3) and lighter (100 lb vs. 350 lb) than the old version and should function nicely on the *R/V Fishawk*, a vessel the size of a small charter fishing boat and costing ~$2,000 per day (vs. $9,000 per day for the *Weatherbird II*).

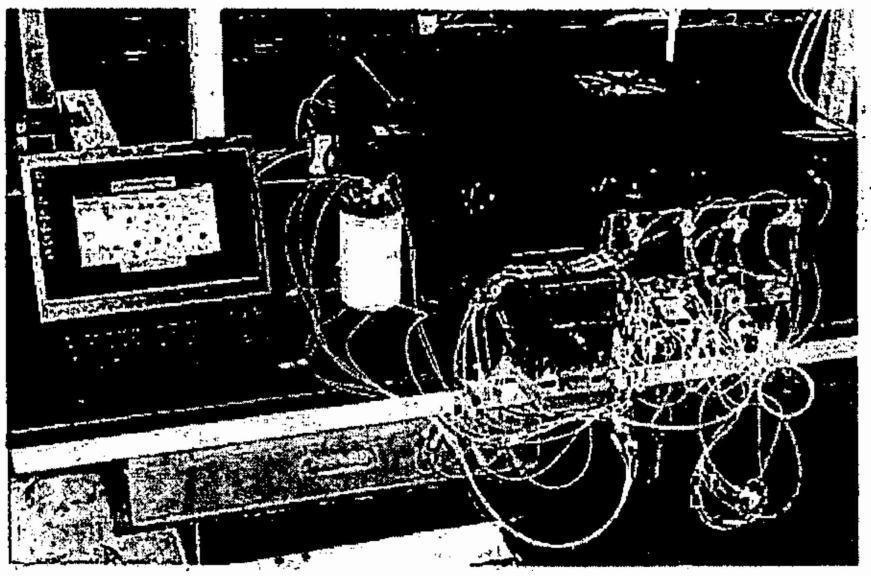

Fig. 6 The new field version of the Masserini-Fanning high sensitivity nitrogen nutrient sensor.

Figure 7 presents the block diagram of the new sensor. Laboratory bench tests indicate that the new version of the nutrient sensor has the same stability and sensitivity as the standard version for two reasons: (1) it uses the proven technology of the AUV version of the sensor and (2) adequate cooling was provided in the form of aluminum heat sinks in the framework and a fan. Whenever possible as the new version was built, upgrades of individual components (12-channel pump, circuit boards, relay controllers, etc.) were installed, to increase stability and sensitivity

even further. Typical strip charts from calibration runs and the regression data from these runs is presented in Fig. 8 and 9, respectively.

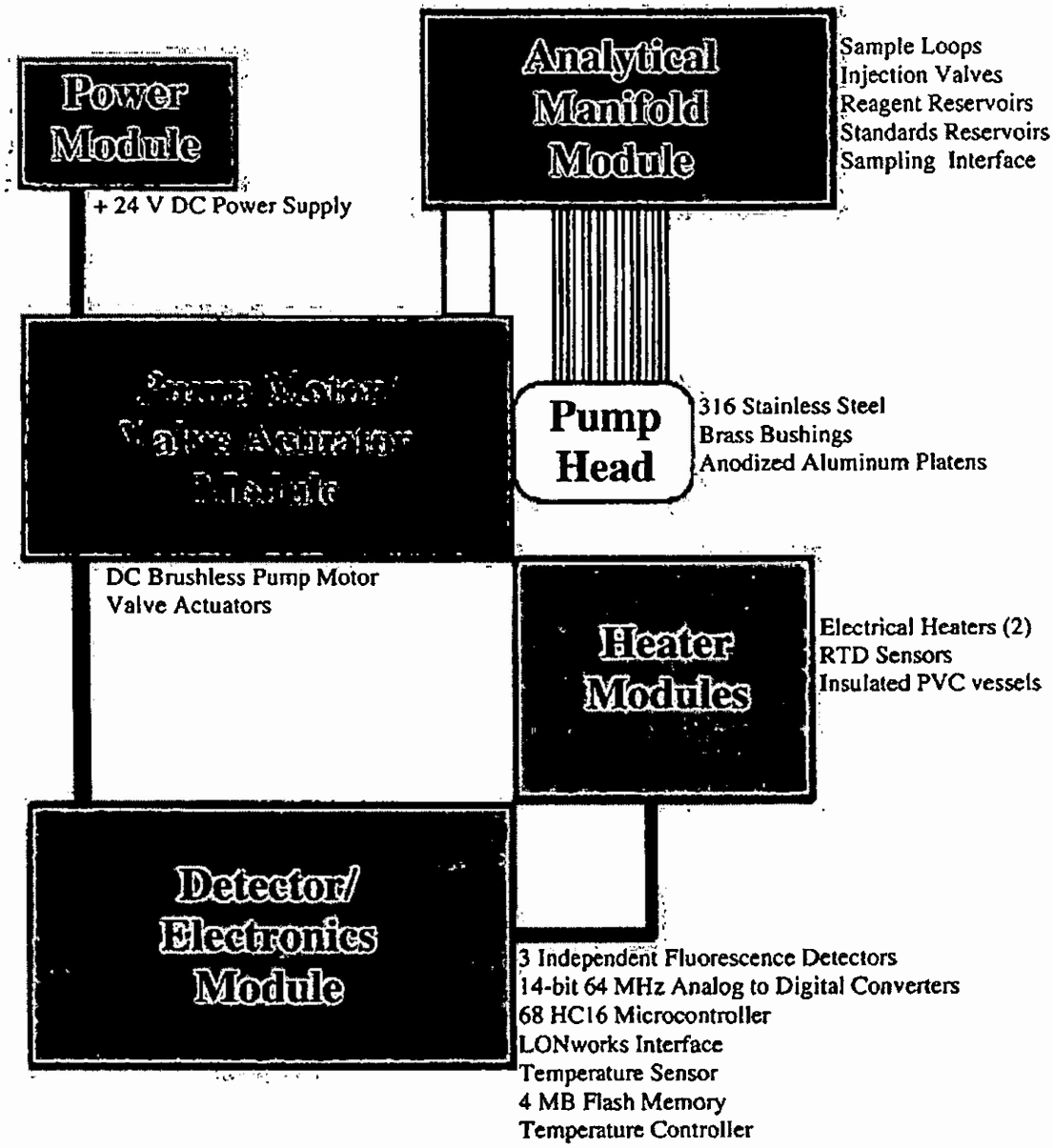

Fig. 7. Block diagram of the compact fluorescent nitrogen nutrient sensor.

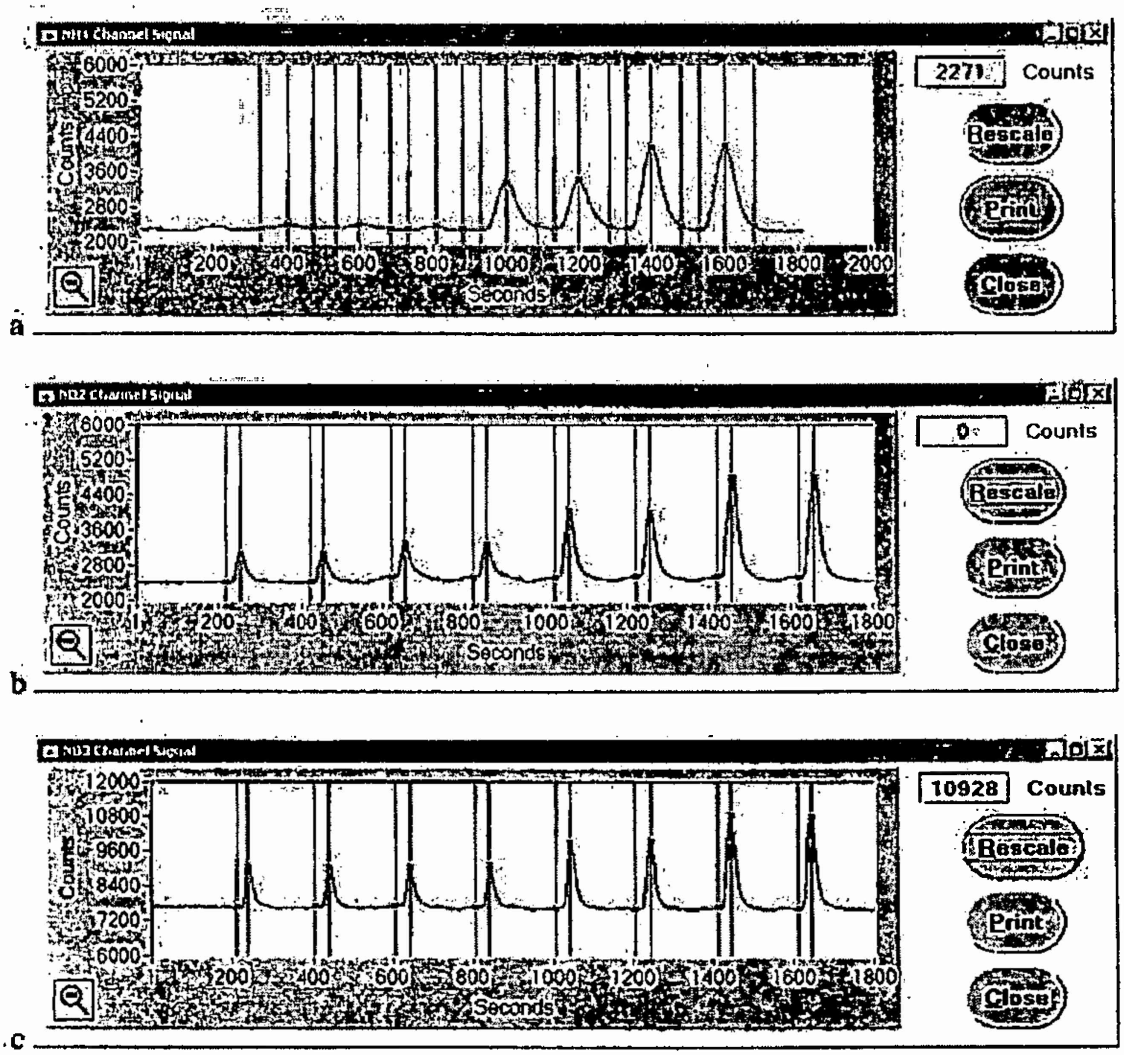

Fig. 8 Peak records for fluorescent ammonium (a), nitrite (b), and nitrate+nitrite (c) calibration standards. The first two peaks in the records are reagent blanks. The next six peaks are duplicates of spiked low nutrient seawater samples corresponding to 0, 500, and 1000 nM for ammonium and nitrite and 0, 1000, and 2000 nM nitrate+nitrite. Red and pink vertical lines indicate where the background or baseline fluorescence is measured for each sample and blue vertical lines are where the peak height for each sample is taken

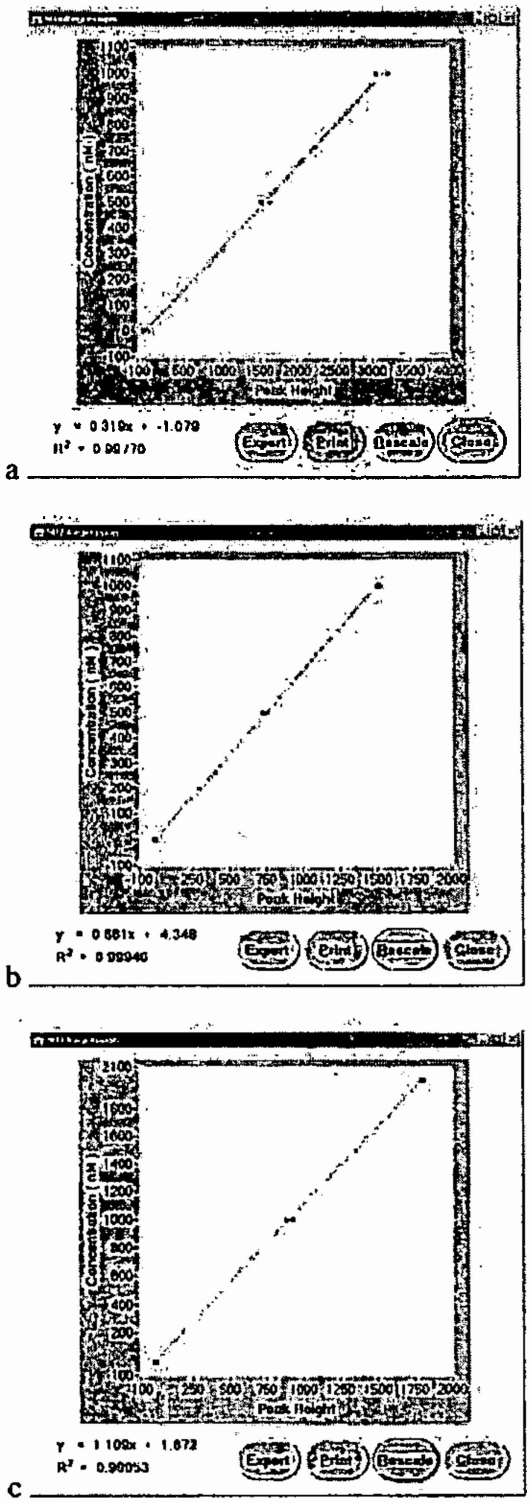

Fig. 9 Calibration curves for the fluorescent ammonium (a), nitrite (b), and nitrate+nitrite (c) calibration standards shown in Figure 8.

A two-day field test of the instrument was conducted in the summer on the *Weatherbird II* where the instrument was connected to acid-cleaned high-density polyethylene tubing married to a Vectran line and connected to a stainless-steel "fish" that was dragged behind the ship. An air-driven, chemically pure suction pump sucked seawater through the tubing up into the ship's laboratory where it was subsampled and measured for nitrate, nitrite, and ammonium. The new sensor performed up to expectations, achieving detection limits of less than 20 nM for ammonium and nitrite and less than 50 nM for nitrate. During the field test, the system detected an ammonium peak of 880 nanomolar, which contrasted sharply with most of the ammonium values, which were ≈ 100 nanomolar (the "background" ammonium values found in these waters by Fanning et al., (2012)). This ammonium peak, more than twice the highest peak found before, supports the prediction made by Fanning et al. that summertime might be the best time to find ammonium peaks that might provide stronger labels or tracers for these water masses.

The sensor will play critical roles in support of remote sensing operations from fixed moorings or platforms: recalibration. Nutrient-measuring devices that are often proposed for long-term autonomous deployment on these installations present some serious difficulties. Most of the autonomous devices utilize reagents to react with nutrients, and reagents can become unstable over periods of days to months. Recalibration is thus necessary, but, unfortunately, internal nutrient recalibration standards can become unstable as well. Even if nutrient-measuring devices on fixed monitoring stations worked "perfectly," the data they generate cannot yield an adequate picture of the nutrient distribution patterns in the waters between the stations. Periodic surveys by an instrument like the "blue box" in Fig. 6 can easily provide the needed data. It can perform both calibrations and surveys on regularly scheduled transects conducted close to the installations and/or between them. The transects could be conducted via a small, cheap-to-operate vessel.

Long-Term Monitoring of Dissolved Nitrate in Ocean Water by an ISUS Ultraviolet Sensor

As mentioned under Long-Term Goals, we began the evaluation of the use of an Satlantic (now part of SeaBird Scientific) ISUS ultraviolet sensor for nitrate ion in seawater. The powerful advantage of this unit is that it uses the UV absorption by nitrate as the detection technique and thus requires no internal standards, reagents, or blank solutions that can degrade over time and make the results uncertain. A disadvantage, however, is that its detection limits (~2 μmolar) are not very sensitive for much of the upper ocean, including many coastal regions. Also the sensing unit is susceptible to biofouling. Our objective was to deploy an ISUS and ascertain its analytical and monitoring capabilities. The approach for this objective centered on maintaining the sensor array installed on the Hillsborough River as well as collecting discrete water samples to evaluate the accuracy and response of the ISUS UV nitrate sensor. Real time ISUS data are telemetered and displayed at http://comps.marine.usf.edu/index?view=station&id=UTP. Figure 10 presents the nitrate time course from the Hillsborough River station in Tampa Bay for the first half of 2009. For the first two months that ISUS #161 was deployed, its data were in reasonable agreement with the discrete colorimetric nitrate analyses performed on a Technicon AAII autoanalyzer. Later in the year ISUS #161 was replaced by another ISUS (#075), and a significant difference was found between the discrete samples and the ISUS-derived concentrations. This shift was related to an instrumental calibration offset. We have found that

the contribution from dissolved organic matter (DOM) to the UV absorption measured by the ISUS causes its nitrate values to be overestimates of the actual nitrate concentrations. Since 2009, we have continued this ISUS evaluation, including work on a means of calibrating the ISUS using standard nitrate additions to water with high DOM in order to correct for this offset. We have not found out how to make the ISUS work well for the monitoring purposes we

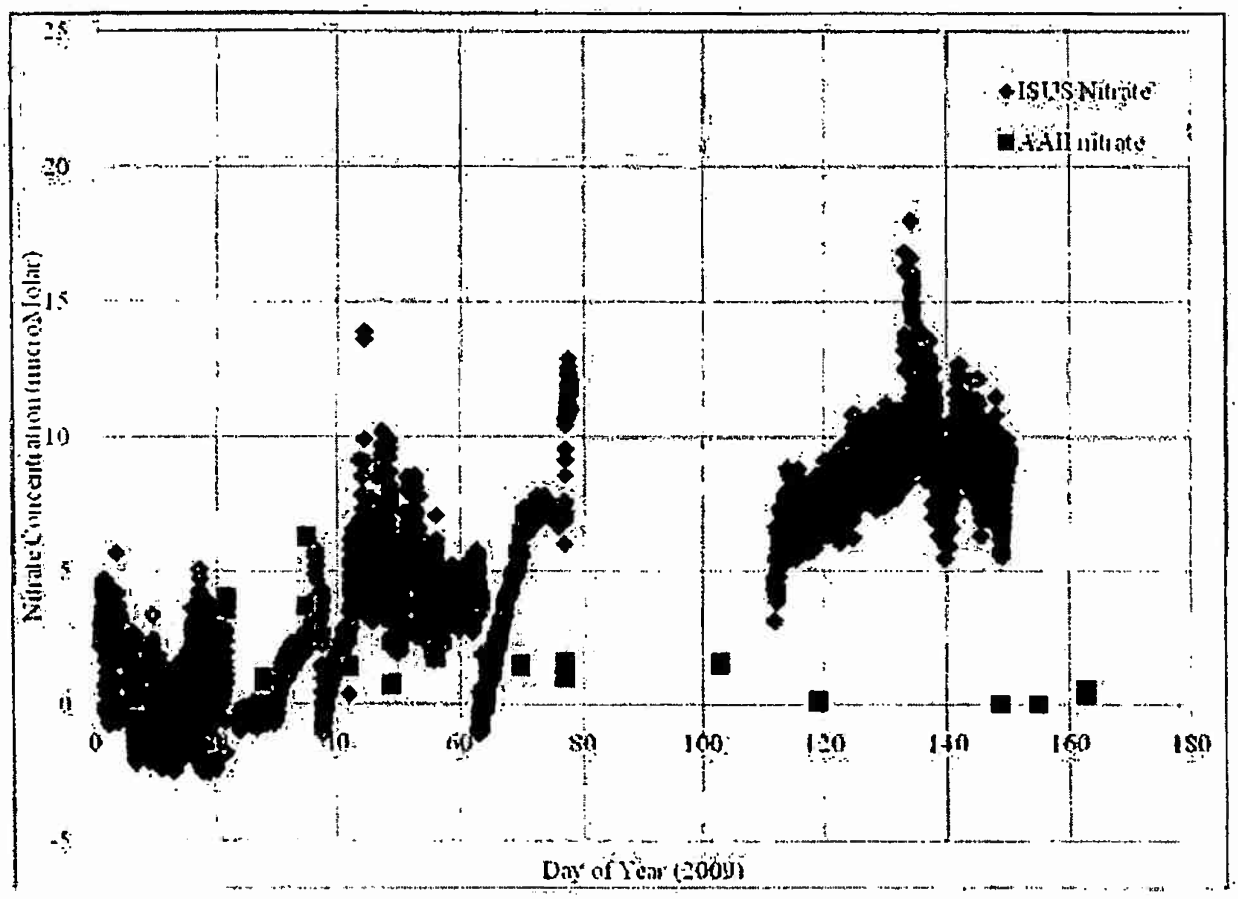

Figure 10. Nitrate time course measured at the Hillsborough River installation for the first half of 2009. Blue data points are ISUS-derived nitrate concentration, and red data points are discrete water sample nitrate values used to evaluate the ISUS response. After approximately three months the first ISUS deployed failed, and a second unit was deployed on day 111. This unit had a higher offset due to an internal calibration error.

intended. Internal component failure (like the shutter controlling the signal) happen too frequently. Biofouling is a constant problem. Data acquisition via the Web is sometimes erratic. But, we have at times seen some intersting nitrate signals which were coherent in time with reasonably smooth trends that matched salinity or other variables. So we continue with this field analytical monitoring research.

References

Dortch, Q. 1990. The interaction between ammonium and nitrate uptake in phytoplankton. *Marine Ecol. Prog. Ser.* **61**, 183-201.

Fanning, K.A., R. Masserini, J.J. Walsh, R. Wanninkhof, K. Sullivan, and J.I. Virmani. 2012. Wind forcing, ammonium events, and the nutrient regime in the surface ocean, (to be submitted)

Gordon, L.I., Jennings, J.C. Jr., Ross, A.A., and Krest, J.M. 1993. A suggested protocol for continuous flow automated analysis of seawater nutrients (phosphate, nitrate, nitrite and silicic acid in the WOCE Hydrographic Program and the Joint Global Ocean Fluxes Study. In: WOCE Hydrographic Program Office, Methods Manual WHPO 90-1

Hildebrand, M. 2005. Cloning and functional characterization of ammonium transporters from the marine diatom cylindrotheca fusiformis (bacillariophyceae). *J. Phenol.* **41**, 105-113.

Johnson, M. T., P. S. Liss, T. G. Bell, T. J. Lesworth, A. R. Baker, A. J. Hind, T. D. Jickells, K. F. Biswas, E. M. S. Woodward, and S. W. Gibb. 2008. Field observations of the ocean-atmosphere exchange of ammonia: fundamental importance of temperature as revealed by a comparison of high and low latitudes, *Global Biogeochem. Cycles.* **22**, GB1019, doi:10.1029/2007GB00309

Masserini, R. T. and K. A. Fanning. 2000. A sensor package for the simultaneous determination of nanomolar concentrations of nitrite, nitrate, and ammonia in seawater by fluorescence detection. *Mar. Chem.* **68**, 323-333.

Martin, A. P. 2003. Phytoplankton patchiness, the role of lateral stirring and mixing. *Prog. in Oceanog.* **57**, 125-174.

Mulholland, M. R., P. W. Bernhardt, C. A. Heil, D. A. Bronk, and J. M. O'Neil. 2006. Nitrogen fixation and release of fixed nitrogen by *Trichodesmium* spp. in the Gulf of Mexico. *Limnol. Oceanog.* **51**, 1762-1776.

Neumann, G and W.J. Pierson. 1966. *Principles of Physical Oceanography* (Prentice-Hall, Inc., Englewood Cliffs, NJ.

Solorzano, L. and J. H. Sharp. 1980. Determination of total dissolved nitrogen in natural waters. *Limnol. Oceanogr.* **25**, 751-754.

Valderama, J .C. 1981. The simultaneous analysis of total nitrogen and total phosphorus in natural waters. *Mar. Chem.* **10**, 109-122.

Vecchi, G. A. and B. J. Soden. 2007. Increased tropical Atlantic wind shear in model projections of global warming. *Geophys. Res. Lett.* **34**, L08702, doi:10.1029/2006GL028905

Virmani, J. I. and R. H. Weisberg. 2005. Relative humidity over the West Florida Continental shelf. *Monthly Weath. Rev.* **133**, 1671-1686.

Wanninkhof, R. 1992. Relationship between wind speed and gas exchange over the ocean. *J. Geophys. Res.* **97**, 7373-7382.

Weisberg, R. H., Y. Liu, and D. A. Mayer. 2009. West Florida Shelf mean circulation observed with long-term moorings. *Geophys. Res. Lett*, **36**, doi:10.1029/2009GL040028.

Yool, A., A. P. Martin, C. Fernández, and D. R. Clark. 2007. The significance of nitrification for oceanic new production. *Nature* **447**, 999-1002 doi:10.1038/nature 05885